ISTANBUL TECHNICAL UNIVERSITY ★ GRADUATE SCHOOL OF SCIENCE
ENGINEERING AND TECHNOLOGY

NEURAL NETWORK BASED MULTI-CARRIER RECEIVER DESIGN AND DOPPLER ESTIMATION

M.Sc. THESIS

Yasin YILDIRIM

Electronics and Communication Engineering Department

Telecommunication Engineering Programme

JULY 2020

ISTANBUL TECHNICAL UNIVERSITY ★ GRADUATE SCHOOL OF SCIENCE
ENGINEERING AND TECHNOLOGY

NEURAL NETWORK BASED MULTI-CARRIER RECEIVER DESIGN AND DOPPLER ESTIMATION

M.Sc. THESIS

Yasin YILDIRIM
(504171337)

Electronics and Communication Engineering Department

Telecommunication Engineering Programme

Thesis Advisor: Prof. Dr. Hakan Ali Çırpan
Co-advisor: Dr. Sedat Özer

JULY 2020

İSTANBUL TEKNİK ÜNİVERSİTESİ ★ FEN BİLİMLERİ ENSTİTÜSÜ

YAPAY SİNİR AĞI TABANLI ÇOK TAŞIYICILI ALICI TASARIMI ve DOPPLER KESTİRİMİ

YÜKSEK LİSANS TEZİ

Yasin YILDIRIM
(504171337)

Elektronik ve Haberleşme Mühendisliği Anabilim Dalı

Telekomünikasyon Mühendisliği Programı

Tez Danışmanı: Prof. Dr. Hakan Ali Çırpan
Eş Danışman: Dr. Sedat Özer

TEMMUZ 2020

Yasin YILDIRIM, a M.Sc. student of ITU Graduate School of Science Engineering and Technology 504171337 successfully defended the thesis entitled “NEURAL NETWORK BASED MULTI-CARRIER RECEIVER DESIGN AND DOPPLER ESTIMATION”, which he/she prepared after fulfilling the requirements specified in the associated legislations, before the jury whose signatures are below.

Thesis Advisor :	**Prof. Dr. Hakan Ali Çırpan** Istanbul Technical University	....
Co-advisor :	**Dr. Sedat Özer** Bilkent University	....
Jury Members :	**Prof. Dr. Ender Mete Ekşioğlu** Istanbul Technical University	....
	Prof. Dr. Selçuk Paker Istanbul Technical University	....
	Dr. Mehmet Başaran Vodafone Future Lab	....

Date of Submission : **15 June 2020**
Date of Defense : **02 July 2020**

To my family,

FOREWORD

The work presented in this thesis was conducted during my M.Sc. study at Telecommunication Engineering Program of Electronics and Communication Engineering Department in Istanbul Technical University Graduate School of Science Engineering and Technology. I would like to take this opportunity to acknowledge all the people who have supported me.

First and foremost, I would like to express my gratitude to my supervisor Prof. Dr. Hakan Ali ÇIRPAN for giving me a chance to be a graduate student. I greatly appreciate his excellent guidance, trust and support during my master degree process. I also want to express my gratitude to Dr. Sedat ÖZER for steering me into this interesting research topic and continuous support throughout this research work. I am grateful to him for his generosity in sharing his expertise and time in our frequent discussions. I would like to thank Asst. Prof. Ali GÖRÇİN for encouraging me to help me to build a strong research mindset with his continuous pushing and high expectations along with valuable feedbacks and moral support. Last, but not least, I want to express my utmost gratitude to my family.

July 2020 — Yasin YILDIRIM
(Research Assistant)

TABLE OF CONTENTS

Page

ABBREVIATIONS

RF	: Radio Frequency
LPF	: Low Pass Filter
AWGN	: Additive White Gaussian Noise
BER	: Bit Error Rate
SNR	: Signal to Noise Ratio
BPSK	: Binary Phase Shift Keying
QPSK	: Quadrature Phase Shift Keying
dB	: Decibel
RMS	: Root Mean Square
ISI	: Inter Symbol Interference
ICI	: Inter Carrier Interference
CLT	: Central Limit Theorem
LOS	: Line of Sight
MLP	: Multi-Layer Perceptron
CNN	: Convolutional Neural Network
ReLu	: Rectifier Linear Unit
Adam	: Adaptive Moment Estimation
ROC	: Receiver Operating Characteristics
PR	: Precision-Recall
MDS	: Maximum Doppler Shift
SCF	: Spectral Correlation Function
MSE	: Mean Square Error
MCM	: Multi-Carrier Modulation
LTE	: Long Term Evolution
FFT	: Fast Fourier Transform
IFFT	: Inverse Fast Fourier Transform
CP	: Cyclic Prefix
FDE	: Frequency Domain Equalization
PAPR	: Peak to Average Power Ratio
ADC	: Analog to Digital Converter
DAC	: Digital to Analog Converter
LFDMA	: Localized Frequency Division Multiple Access
IFDMA	: Interleaved Frequency Division Multiple Access
SSE	: Symbols-Spaced Equalizer
FSE	: Fractionally-Spaced Equalizer
OOB	: Out of Band

LIST OF TABLES

Page

LIST OF FIGURES

Page

NEURAL NETWORK BASED MULTI-CARRIER RECEIVER DESIGN AND DOPPLER ESTIMATION

SUMMARY

Recently, various industry applications have been developed in line with the needs of the society in accordance with the changing lifestyle. Applications such as virtual and augmented reality, remote surgery, fully autonomous systems and holographic reflection will cause various changes in communication systems. Current technology is insufficient to meet the increasing traffic needs demanded by these applications. Also, a reduction in the amount of delay is required for these applications. In this context, communication systems must be updated with new generation techniques.

Artificial intelligence is one of the rapidly developing fields of computer science in the past decade. This study includes telecommunication applications of AI discipline. In the first stage of the thesis, the receiver design of single carrier systems has been made with artificial neural network. This section is an introduction for the purpose of interpreting and reasoning the artificial neural network structure in multi-carrier systems. In the second stage of the thesis, artificial neural network based receiver design is focused for multi-carrier wireless communication system. First, a modular unified transmitter structure is designed that combines orthogonal and non-orthogonal multi-carrier systems. Symbols are produced through the modulation matrix at the transmitter. These symbols are then transmitted from the transmitter to the receiver, passing through multi-path wireless channel. 1D CNN, 2D CNN and MLP based architectures are used to detect symbols sent from the transmitter. In this study, 2D CNN architecture was evaluated for the first time. In addition, in previous studies, channel equalization is performed as a preprocess in the receiver, while in this study, detection procedures are performed without channel equalization in the receiver design. Likewise, in the previous studies, after the symbols passed from the channel equalization, they are subjected to coarse detection and given to the neural network. The performances of the algorithms are evaluated on OFDM and GFDM multi carrier systems. The results are compared with classical techniques such as MF, ZF, MMSE. In the third stage of the thesis, Doppler frequency shift, which is an important parameter of the wireless channel and significantly affects the performance of the wireless communication system, has been detected with SCF and artificial neural network without any prior knowledge. Within the scope of the study, it is explained how to estimate the Doppler frequency without the need for prior knowledge or signal and it have made blind for the first time in the literature. SCF is used to extract the statistics of the signal, and Regression CNN is used to estimate the parameter with these statistics. The performance of the algorithm is tested with a dataset containing analog modulations and results are shown.

YAPAY SİNİR AĞI TABANLI ÇOK TAŞIYICILI ALICI TASARIMI ve DOPPLER KESTİRİMİ

ÖZET

Son zamanlarda toplumun değişen yaşam tarzına uygun olarak ihtiyaçlar kapsamında çeşitli endüstri uygulamaları geliştirilmektedir. Sanal ve arttırılmış gerçeklik, uzaktan ameliyat, tam otonom sistemler ve holografik yansıma gibi uygulamalar haberleşme sistemlerinde çeşitli değişimlere yol açacaktır. Mevcut teknoloji bu uygulamaların talep ettiği artan trafik ihtiyacını karşılamakta yetersiz kalmaktadır. Bununla birlikte bu uygulamalar için gecikme miktarında azalma gerekmektedir. Bu bağlamda haberleşme sistemleri yeni nesil tekniklerle güncellenmek durumundadır.

Yapay zeka son on yılda bilgisayar biliminin hızla gelişen alanlarından biridir. İnternet kullanımının artmasıyla veri üretimi artmıştır. Bununla birlikte yüksek miktardaki verileri kullanarak anlamlı sonuçlar çıkarmaya ihtiyaç doğmuştur. Bu ihtiyacı klasik yöntemler işlem karmaşıklığı ve genelleştirememe gibi sorunları nedeniyle karşılamada yetersiz kalır. Derin öğrenme yardımıyla üretilen büyük veriler anlamlandırılarak istenen çıktı elde edilebilir. Bu sebeple derin öğrenme telsiz iletişimde kullanımı diğer disiplinlerde olduğu gibi ilgi çekici haline gelmiştir. Dolayısıyla, araştırmacıların ilgisini çekmiş kanal kestirimi, kanal kodlama, ağ katmanı en iyileştirmesi gibi alanlarda kulanımını ile ilgili çalışmalar yapılmıştır.

Bu çalışma AI disiplininin telekomünikasyon uygulamalarını içermektedir. Gelecek nesil fiziksel katman yapısına uygun olarak yapay zeka tabanlı alıcı yapısı ve kör en büyük doppler frekansı kestirim algoritması uygulamaları üzerine çalışılmıştır. Bu bağlamda, CNN ve MLP yapılarını kullanan derin alıcı ve SCF ve CNN yapılarını kullanan doppler parametre tahmin algoritması tartışılmıştır.

Tezin ilk aşamasında tek taşıyıcılı sistemlerin alıcı tasarımı yapay sinir ağı ile yapılmıştır. Bu kısım ikinci bölümde tartışılacak olan çok taşıyıcılı sistemlerde yapay sinir ağı yapısını anlamlandırma ve yorumlama amacıyla giriş niteliğindedir. Tasarlanan sistemde tek taşıyıcılı PSK modülasyonuna uğramış vericide üretilen semboller kanaldan geçerek alıcıda yapay sinir ağı ile çözülür. Alıcıda yoğun ağ yapısı bilinen sembollerle eğitilmiştir. Yapay sinir ağının performansı karşılaştırmak amacıyla klasik yapı olarak kullanılan en büyük olabilirlik kriteri ile karşılaştırılmıştır. Bu yöntem yıldız diyagramdaki hangi sembolün alınan işarete en yakın olduğu belirleyenerek tespit gerçekleştirir ve tek taşıyıcılı alıcı problemi için optimum alıcıdır. Bulunan sonuçlar klasik alıcısının BER performansı ile örtüşmektedir. Bunun sebebi sinir ağını karar bölgesi eğitim sonunda optimum kararla neredeyse aynı olmasıdır.

Tezin ikinci aşamasında çok taşıyıcılı kablosuz haberleşme sistemi için yapay sinir ağı tabanlı alıcı tasarımına odaklanılmıştır. Öncelikle dik olan ve dik olmayan çok taşıyıcılı sistemleri birleştiren modüler birleşik bir verici yapısı tasarlanmıştır. Vericide semboller modülasyon matrisi aracılığı ile üretilir. Modülasyon matrisi farklı modülasyon teknikleri için farklı operasyonlar ihtiva eder. Örneğin OFDM iletişim sistemi için N-nokta IFFT işlemi gerçekleştirir. GFDM iletişim sistemi için örnekleme, darbe şekillendirme ve frekans kaydırma işlemlerini gerçekleştirir. Üretilen semboller kablosuz kanaldan geçerek alıcıya ulaşır. Kanal çok yollu sönümlemeli kanal olarak modellenmiştir. Temel bantta alınan semboller gerçel ve sanal bileşene sahip komplex verilerden oluşur. Semboller kanaldan geçmesi sebebiyle bozunumlara uğramıştır. Alıcıda yapay sinir ağı ile özellik çıkarma ve sınıflandırma işlemleri yapılarak kanalın bozucu etkileri yok edilmeye çalışılır. Dolayısıyla yapay sinir ağı sembol tespit algoritması olarak değerlendirilir. Sinir ağı eğitimininde denetimli öğrenme benimsenmiştir. Ağ eğitim aşamasında etiket olarak kabul edilen bilinen semboller ile eğitilmiştir. Yapay sinir ağı tabanlı alıcı olarak üç tür yapı tasarlanmıştır. İlk algoritmada, gerçel ve sanal bileşenleri olan semboller seri hale getirilip MLP yardımıyla tespit işlemi gerçekleştirilir. Benzer şekilde bir boyutlu CNN tasarımında sembollerin gerçel ve sanal bileşenleri seri hale getirilip sinir ağına verilir. Üçüncü algoritmada ise gerçel ve sanal bileşenleri paralel hale getirilip iki boyutlu CNN sinir ağına verilir. Yapılan çalışmada iki boyutlu CNN mimarisi ilk kez değerlendirilmiştir. Ayrıca daha önceki çalışmalarda alıcıda ön işlem olarak kanal denkleştirme gerçekleştirilirken, bu çalışmada alıcı tasarımında kanal denkleştirme olmadan tespit işlemleri yapılır. Aynı şekilde daha önceki çalışmalarda kanal denkleştirmeden gecen semboller sonrasında kaba tespit işlemine tabi tutularak sinir ağına verilir. Bu çalışmada alıcıya ulaşan semboller direk olarak algoritmanın girişini besleyerek gönderilen semboller tespit edilir. Bu işlemler dolayısıyla önceki çalışmalarda önerilen sinir ağı tabanlı yaklaşımlara göre karmaşıklık azaltılmıştır. Ayrıca eğitim yüksek çevrim sayısı ile gerçekleştirilir. Öğrenme aktarımı yardımıyla daha önceki eğitim ağırlıkları kullanılarak çevrim sayısı azaltılıp eğitim süresi azaltılmıştır. Aynı zamanda bu yaklaşım alıcın kanal etkilerindeki değişime karşı oldukça uyumlu olarak çalışmasını sağlar. Ayrıca, dik olmayan çok taşıyıcılı GFDM benzeri modülasyonlar için sinir ağı tabanlı yaklaşım karmaşıklığı azaltmaktadır ve algoritmalar tak çıkar sistemi olan modüler olarak üretilen bir yapıdadır. Algoritmaların performansları OFDM ve GFDM çok taşıyıcılı sistemleri üzerinde değerlendirildilmiştir. Sonuçlar MF, ZF, MMSE gibi klasik tekniklerle karşılaştırılmıştır. Ön simülasyonlarda, farklı hiper parametreleri olan farklı katmanlar içeren ağlar test edilmiştir ve sonuçlarda gösterildiği gibi, sığ ağlar en iyi performansı vermiştir. Hem OFDM hem de GFDM deneyleri için, 2 + 1 ağlar CNN mimarı arasında en iyi performansı vermiştir. MLP tabanlı algoritma OFDM için biraz daha iyi performans verebilirken, bellekte tutulması için daha fazla parametre gerektirebilir. Başka çalışmalarda farklı ağ mimarileri farklı modülasyonlar için performans analizine odaklanılabilir.

Tezin üçüncü aşamasında kablosuz kanalın önemli bir parametresi olan ve kablosuz iletişim sisteminin performansını önemli ölçüde etkileyen Doppler frekansı kayması yapay sinir ağı hiçbir ön bilgi kullanılmadan tespit çalışması yapılmıştır. Doppler frekansı radardaki hedef hızlarını ölçmek, sabit ve hareketli hedefleri birbirinden ayırmak gibi uygulamarda kullanılan önemli bir parametredir. Buna karşın etki kablosuz kanaldan geçen sembollerin alıcıda tespiti büyük oranda zorlaştırır. Etkiyi tamamen yok etmek hareketli nesnelerin durdurulması ile mümkün olmaktadır. Pratikte bu yaklaşım gerçekci değildir. Bunun yerine Doppler frekansı kaymasını ve izgesini tespit edip etkileri azaltıcı algoritmalar geliştirmek gerçekci bir yaklaşım olacaktır. Doppler tahmini, önceki çalışmalarda iletilen sinyaller, bilinen sinyaller veya bilinen önceki bilgilerle yapılmıştır. Çalışma kapsamında, önceden bilgi veya sinyale ihtiyaç duymadan doppler frekansının nasıl tahmin edileceği açıklanmaktadır ve literatürde ilk kez kör olarak yapılmıştır. Vericiden üretilen işaretin modülasyon türü, modülasyon parametreleri ve kodlama gibi çeşitli özellikleri gözlemci tarafından bilinmemektedir. Bunun yanı sıra doppler etkisi ile beraber kanalın diğer bozucu etkilerine maruz kalan sembollerin değişimide sisteme serbestlik derecesi kazandırmaktadır. Bu noktada gözlemci doppler frekansı kaymasına duyarlı ve diğer tüm parametrelere karşı duyarsız davranan algoritma ile tespit işlemi gerçekleştirmesi gerekir. Ayrıca geliştirilen algoritma farklı gürültü seviyelerinde sağladığı istatistiği korumak durumundadır. Bu sebeple çeşitli denemelerden döngüsel korelasyona dayalı SCF algoritmasının işaretin ve kanalın tüm etkilerine karşı minimum duyarlı ve doppler frekansına oldukça duyarlı olduğu gözlemlenmiştir. Ayrıca fonksiyon frekans düzleminde çalışması sebebiyle AWGN etkisiyle istatistiksel özellikleri oldukça az etkilenmektedir. Bu fonksiyonu hesaplamada FAM yönteminden yararlanılmıştır. Doppler frekansı artması SCF düzleminde yayılmaya yol açar. Yayılmanın miktarının ölçülmesi ile frekans kayması miktarı üzerinde tahminlerde bulunulabilir. Çıktıyı işlemek için Regresyon CNN ağı kullanılmıştır. Fonksiyonun çıktısı frekans ve döngüsel frekans düzlemini içeren iki boyutlu bir matris olması sebebiyle CNN ağ yapısının çalışma prensiplerine uygun olmaktadır. Bu kapsamda analog modülasyonları içeren bir veri kümesi oluşturulup algoritma test edilmiştir ve algoritmanın performansı gösterilmiştir. Daha ileri bir çalışmada, performansı artırmak için ön bilgileri dikkate almaya odaklanılabilir.

1. INTRODUCTION

In recent years, the demand for next generation telecommunication technologies has been increasing rapidly in order to meet the ever-increasing consumer needs. On the other hand, due to its performance, deep learning (DL) has been used in many applications in many fields today. Within the scope of this thesis, DL based receiver design strategies and a parameter estimation algorithm has been studied.

1.1 Summary of The Related Work

This thesis studies various DL strategies and their performance in receiver design for wireless communication systems using multi-carrier waveforms. In that context, deep receiver architectures using CNN and MLP structures and Doppler parameter estimation algorithm using SCF and CNN structures are discussed. Consequently, this section summarizes the relevant works from the literature.

Modern wireless communication systems heavily rely on multi-carrier wave-forms. Orthogonal Frequency Division Multiplexing (OFDM) [1], Generalized Frequency Division Multiplexing (GFDM) [2], Filter Bank Multi-Carrier (FBMC) and Universal Filtered Multi-Carrier (UFMC) [3] are examples for multi-carrier wave-forms. Such variability in wave-forms, brings up the need for using unified receiver architectures that are flexible enough to be used for different multiple wave-forms. For example, a receiver that can be used for both OFDM and GFDM systems would be a great use for wireless communication systems. DL based receiver solutions are such emerging potential solutions in receiver design and there are already DL based receiver designs proposed in the literature as in [4, 5]. Among many DL architectures, Convolutional Neural Networks (CNNs) have revolutionized multiple research fields (as in computer vision, natural language processing). That is due to the fact that CNNs provide significant performance improvements, when compared to the classical approaches in many applications. However, their use in the receiver design for wireless communication remains limited. The literature for the receiver design mainly focused on designing deep architectures using fully-connected (dense) layers. There are not many works using 2D CNNs in the literature. However, CNNs showed their use in spatial (2D) datasets already. In communication systems, it is essential to deal with complex numbers and complex numbers can also be represented and considered as 2D (spatial) data. Consequently, a 2D CNN dealing with spatial relations among the data points can be useful in the receiver design. In this thesis, it is analyzed and reported the performance of 2D CNNs in receiver design for wireless systems using multi-carrier wave-forms. Among multiple carrier types, it is focused on studying the performance of 2D CNNs on OFDM and GFDM systems in the experiments. Classical GFDM receivers are known with their heavy computational requirements [6]. While DL architectures can be considered as alternatives for receiver design, as mentioned above, they also introduce their own complexities. The existing based learning architectures using fully connected layers typically require heavier computational complexities, when compared to the use of typical 2D CNNs. Using 2D convolutional layers, provides significant reduction in computational complexity when they replace the larger sized fully connected layers containing the largest number of neurons in the earlier layers; thus they can help reduce the complexities of the used deep architectures. DL-based architectures have been studied in receiver design in the recent literature, however, their properties yet to be fully exploited. While, the researchers started to focus on including deep network architectures in wireless communication systems, the main focus has been on utilizing fully-connected (dense) networks in various communication systems. However, using CNNs can reduce the computational cost when compared to dense networks, while providing similar or better performance to that of dense networks. Dense networks are also known as multi-layer perceptron (MLP) in some literature. In this thesis, it is used both terms interchangeably to refer to the same network type. Fully connected (dense) networks were used in [7] as a part of a communication system. In [8], the authors proposed using dense networks to design receivers for OFDM-based systems. In [9, 10] the authors proposed an OAMP based algorithm that uses training to learn the OAMP parameters in MIMO systems. In [5], a dense network was proposed as detector. In [11], the authors proposed using a dense network for OFDM receivers under the constraint of one-bit complex quantization. Long-short term memory (LSTM) based networks were also used in communication systems. For example, in [12], a deep architecture using LSTM and fully connected layers for OFDM systems was proposed. In [13], deep belief networks and auto-encoders were proposed. Auto-encoders were also proposed in [14]. Similarly, in [15], a fully-connected auto-encoder structure was also proposed. In [16], the authors proposed a detection algorithm that distinguishes multi-carrier signals without prior knowledge. Likewise in [17], the authors proposed two different neural network-based algorithms for detecting signals and determining modulation type.

Most of the above-mentioned work focused on utilizing dense networks in different architectures. In [18], the authors studied the performance of MLPs, CNNs and RNNs for chemical (molecular) communication systems. In [19], the authors proposed an auto-encoder architecture utilizing 2D convolutions for OFDM. The closest work in the literature to study to be described is the work in [4, 20] as they both design a deep receiver for GFDM system using 2D CNNs. The receiver design in [4, 20] contains two detectors: a coarse detector and a fine detector where the coarse detector uses one of the classical methods (e.g., zero force or Minimum Mean Square Estimator) first and then a 2D CNN is proposed to further improve the detection performance. In this thesis, it is investigated on utilizing only a deep architecture that combines both coarse and fine detectors for multi-carrier wave-forms. By reshaping a complex number as 2D number, we can utilize 2D CNNs in the receiver. Therefore, it is studied the performance of 1D and 2D CNNs and compare that to dense networks for communication systems utilizing multi-carrier wave-forms. Furthermore, While the literature using deep architectures mostly focused on OFDM wave-forms, in this thesis, it is studied the performance of using various deep architectures for multiple systems including OFDM and GFDM.

Doppler frequency estimation without prior knowledge was studied . There are some similar studies in the literature. Even if there are studies claiming to be blind in them, these studies are not completely blind. In [21], the authors proposed two Doppler estimation algorithms for underwater acoustic communications to improve the performance of the communication system. The algorithms utilize training sequences located at the beginning and at the end of transmitted data frames. However, the algorithm is limited to the use of PSK modulation and synchronization is required.

In [22], the authors proposed joint Doppler shift and channel estimation algorithm for OFDM transmission systems. The method is based on a time-varying channel model and it utilizes the time-domain training data in successive OFDM symbols. Besides, time domain synchronization is required for this algorithm. In [23], the authors proposed Doppler spread estimation algorithm for OFDM transmission systems. The algorithm utilize phase data of time domain channel estimation over various OFDM blocks and it is restricted for non-Rayleigh fading channel.

1.2 List of Contributions

In the first part of this thesis, deep receiver structures and their performances are studied for multi-carrier transmission systems. The contributions related to that part can be summarizedof the first stage of the thesis can be summarized as follows:

- This thesis introduces a DL based receiver for multi-carrier systems without requiring an additional channel equalization module and eliminates the need for including a coarse detector in the receiver.
- Various 2D CNN receiver architectures and their performance are studied for the design of a deep receiver.
- Neural network and transfer learning is utilized to reduce the complexities for GFDM transmission systems.

In the second part of this thesis, a blind maximum Doppler prediction algorithm has been proposed to detect the strength of Doppler shift effect. The contributions of the second stage of the thesis can be summarized as follows:

- Maximum Doppler estimation is not available in the literature as blind and it has been proposed for the first time in the scope of the thesis.
- CNN based artificial neural network has been used for Doppler estimation.
- SCF was used to extract the feature of the Doppler frequency, and the CNN regression network was used to measure the strength of the Doppler frequency.

2. BACKGROUND

In this section, the concepts that will form the basis for the next chapters are defined. The complex baseband equivalent term used in creating wireless channel and signal models is explained. The preferred basic distributions for wireless channel models are examined.

2.1 Complex Baseband Equivalent

In communication systems, the simulation model is implemented in two ways: *Passband model* and *Equivalent baseband model*. In the passband model, also called *waveform-level simulation model*, the transmitted signal, communication channel and received signal are all represented by samples of wave-forms.

Typically, every details of RF carrier is simulated in the waveform level simulation. Since it requires more samples to represent signal and makes more process to get the desired signal, it consumes more time, memory. Therefore, waveform level simulation model is inefficient way of simulation of communication systems.

For the equivalent complex-baseband model, the required useful value is considered instead of using all unnecessary samples of RF carrier. Thus, the entire symbol, channel and process are represented by a single sample each separately. Therefore, equivalent complex-baseband model is efficient and preferred way of simulation of communication systems.

2.1.1 Complex baseband representation

In any communication system, the transmitter generates information in the baseband and constructs passband waveform. The message to be transmitted is represented as the complex baseband equivalent as follows.

$$\tilde{s} = m_I(t) + jm_Q(t)$$

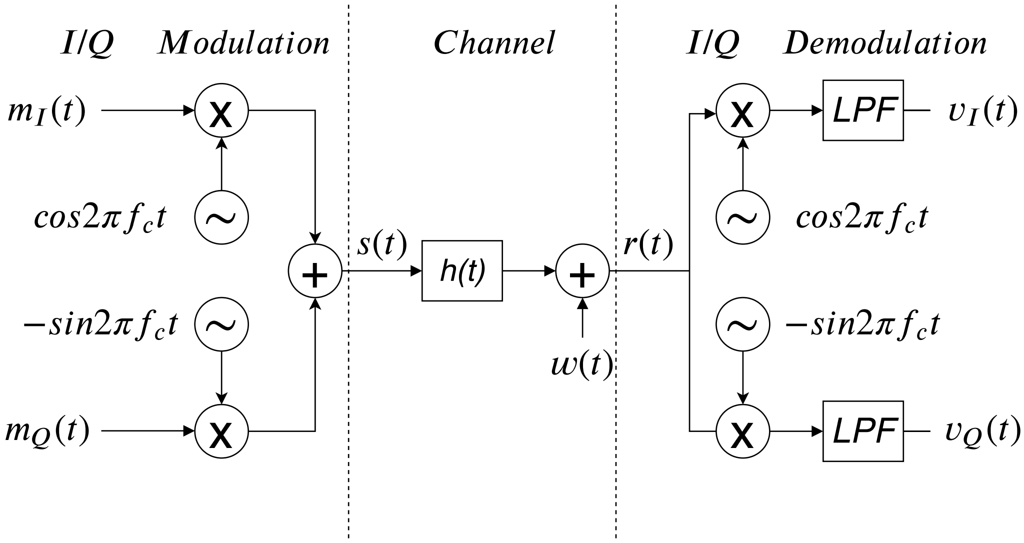

Figure 2.1 : Wireless communication representation

As real part of the symbol is mapped amplitude of the cosine wave, imaginary part of the symbol is mapped amplitude of the sine wave. Resulting waveform is as follows

$$\begin{aligned} s(t) &= m_I(t)\cos(2\pi f_c t) - m_Q(t)\sin(2\pi f_c t) \\ &= a(t)\cos[2\pi f_c t + \phi(t)] \end{aligned}$$

where,

$$\begin{aligned} a(t) &= \sqrt{m_I(t)^2 + m_Q(t)^2} \\ \phi(t) &= \tan^{-1}\left(\frac{m_Q(t)}{m_I(t)}\right) \end{aligned}$$

Entire process is given in Figure 2.1. In the receiver part, demodulation is performed using same carrier signal. Redundant high frequency component is suppressed by LPF and desired complex-baseband signal is obtained.

Likewise wireless channel can be represented by complex-baseband equivalent. Since wireless channel is modeled linear time invariant system, its effect on the modulated signal is represented as linear convolution.

$$r = s * h + w$$

The corresponding complex-baseband equivalent is expressed as

$$(r_I + jr_Q) = (s_I + js_Q) * (h_I + jh_Q) + (w_I + jw_Q)$$

Complex baseband representations of the signals are efficient way of modeling wireless communication systems. Therefore, in this thesis, subsequent models will be modeled as a complex-baseband equivalent.

2.2 Additive White Gaussian Channel

Additive white Gaussian noise is the most used model in information theory. It reduces communication performance in the presence of thermal noise. Thermal noise is caused by the atoms in the receiver electronics vibrating and forming random signals.

The term additive white Gaussian noise (AWGN) originates due to the following reasons:

- *Additive*: The received signal is equal to transmitted signal plus noise, where the noise is statistically independent of the signal.

$$r(t) = s(t) + w(t)$$

- *White*: In the visible spectrum, white color is composed of all frequencies i.e. it is a linear combination of all colors. Similarly, the white noise is called white because it has an equal power in all frequency components in the spectrum. Auto-correlation function of the noise is dirac pulse due to its infinite spectrum, which means it has only correlation own its own, not with its delayed version. As a result of this characteristic, AWGN consists of independent samples.

  The signal of interest is always band-limited in the spectrum. Accordingly, noise components that are not required are filtered out. This leads to transition from ideal to non-ideal case. Likewise, if the signal is sampled, the frequency components of the noise greater than half the sampling frequency are filtered out. Resulting in-band noise after filtering is depicted in Figure 2.2.

  In the spectrum, power of the noise components per unit bandwidth is given as

$$N_0 = \frac{P_w}{B} \tag{2.1}$$

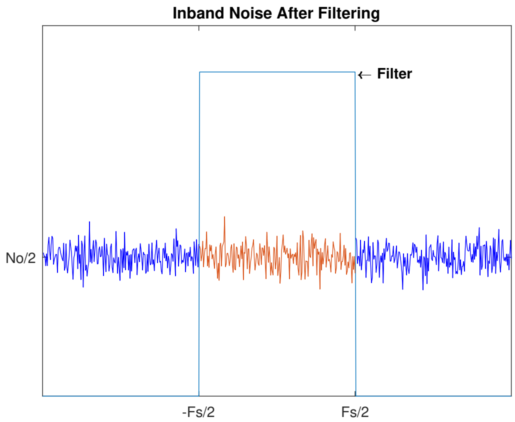

Figure 2.2 : In-band noise after filtering

In-band noise power after sampling with F_s frequency

$$P_w = N_0 \cdot \frac{F_S}{2} \tag{2.2}$$

Consequently, noise power is directly proportional to the sampling frequency, which is twice of the signal bandwidth.

- *Gaussian*: The probability density function of the noise samples is Gaussian distributed with a zero mean. The reason for being its distribution normal originates from the central limit theorem. At its origin, noise is a combination of the distribution of energy produced by many atoms. Normal distribution is observed by combining all these distributions. Probability density function with dependent variable n as follows:

$$f(n) = \frac{1}{\sqrt{2\pi\sigma_n^2}} e^{-\frac{(n-\mu_n)^2}{2\sigma_n^2}} \tag{2.3}$$

where σ_n^2 is the variance and μ_n is the mean of the noise samples.

AWGN channel is one of the most important factors affecting communication performance. Generally, the performance of communication is measured by a bit error curve. Figure 2.3 shows the BPSK performance on the AWGN Channel. Bit error decreases with increasing SNR.

Since the AWGN samples are uncorrelated, the most optimal detection to be made on the receiver when the encoded symbol is sent is to make a prediction with the maximum likelihood decision region. Maximum likelihood receiver is used in the generation of the curve in Figure 2.3.

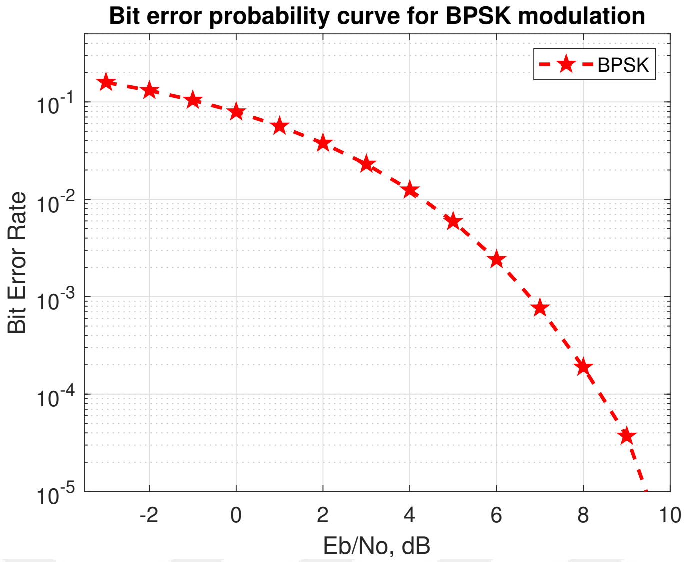

Figure 2.3 : Bit error rate performance for BPSK modulation

The AWGN characteristic is better depicted in the constellation diagram. In Figure 2.4, the 4 cases clearly show the nature of the phenomenon. For the first figure, BPSK symbols without noise is given. Then, AWGN noise with 5, 10, 20 dB SNR is added respectively. Clear distinction appears to start at 10 dB SNR.

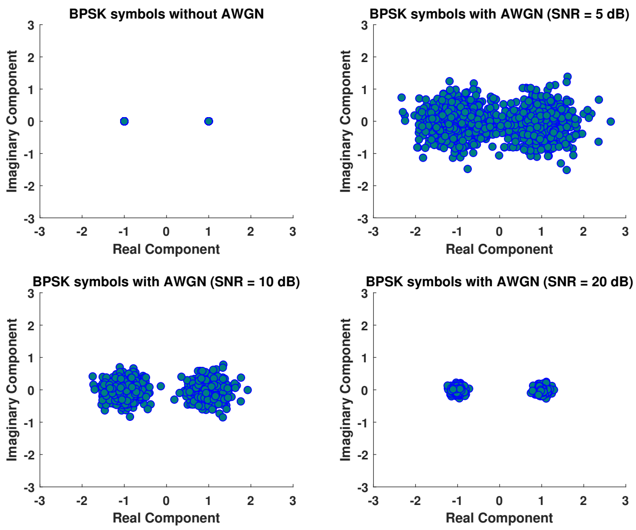

Figure 2.4 : Constellation diagram for BPSK with and without noise

2.3 Main Characteristics of Fading Channels

In a wireless communication environment, the signal is exposed to many effects before it reaches the receiver, such as *multi-path*, *Doppler shift and spread*, *attenuation*, *shadowing*, *absorption*, *refraction*, *diffraction*, *reflection* and *scattering*. These effects can significantly change communications performance. However, in order to eliminate or reduce these effects, studies on statistical model and characterization have been carried out and some methods have been developed.

2.3.1 Slow and fast fading

In the mobile communication environment, there may be moving objects, living things, mobile receivers and transmitters. This mobility causes the Doppler effect. Doppler effect negatively affects frequency domain. It causes the carrier frequency to shift and the frequency components of the signal to spread.

The mobile communication scenario is depicted in Figure 2.5. In the scenario where the transmitter is moving, the center frequency of the transmitted signal increases in the direction of motion, while its center frequency decreases in the opposite direction. In the regions between the direction of movement and the opposite direction, center frequency values vary between the two extreme values. This phenomenon causes the center frequency to shift. Assuming that the frequency-shifting signal reaches the receiver at the same time, the spectrum of the signals with different shifts is summed. Therefore, Doppler spread occurs.

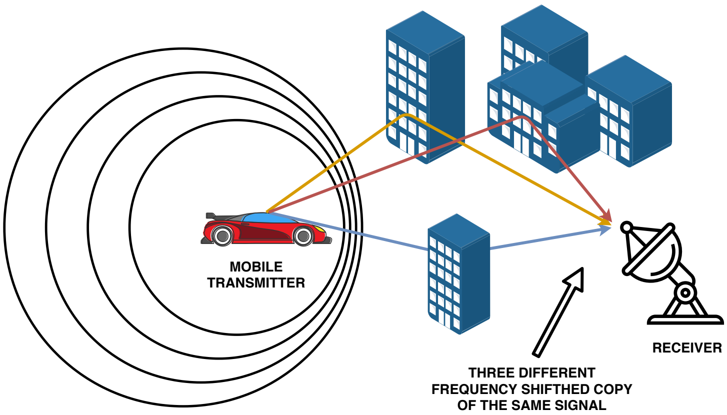

Figure 2.5 : Mobile communication scenario

Time domain and frequency domain are dual. This property leads to the *uncertainty principle*. The uncertainty principle is based on the work of the German physicist Heisenberg. According to Heisenberg, in some cases the position can be known quite well, or in other cases momentum is well known, but there are limits to the accuracy of knowing these two properties at the same time. Similarly, there is the same relationship between time and frequency domain. So there is a relationship between these two domains.

As the Doppler effect causes shifting in the frequency domain, its effects can be examined in the time domain. If there is an excessive shift in frequency, excessive fluctuations occur in time. This property is known as *fast fading*. Likewise, if there is a relative less shift in frequency, less fluctuations occur in time. This property is known as *slow fading*.

The frequency shift that is the result of the Doppler effect causes a constraint in time which is known as *coherence time*. As can be seen in Equation 2.4, the coherence time is inversely proportional to the maximum Doppler shift.

$$T_c \approx \frac{1}{fd_{\max}} \tag{2.4}$$

As a result, if the symbol duration is shorter than the coherence time, slow fading occurs. Similarly, if the symbol duration is greater than the coherence time, fast fading occurs.

2.3.2 Frequency-flat and frequency-selective fading

Another effect that disrupts the signal in the wireless environment is multipath channel fading. Multipath channel means that the signal sent from the transmitter passes through many paths and reaches the receiver at different times. This scenario is depicted in Figure 2.6. As can be seen, copies of the signal sent from the transmitter are reflected from many buildings and reached the receiver. These signal copies, coming at different times, combine at the receiver in a constructive or destructive way. As a result of this phenomenon, some carrier frequencies become stronger while others become weak in the context of the power.

Copies of the symbol reaching the receiver relatively late by passing through the multipath channel combine with the first copies of the next symbol. This disruptive effect is called *Inter Symbol Interference*. As ISI causes interference of symbols, it also makes it difficult to demodulate the signal at the receiver. Hence, ISI is one of the main distortions to be avoided.

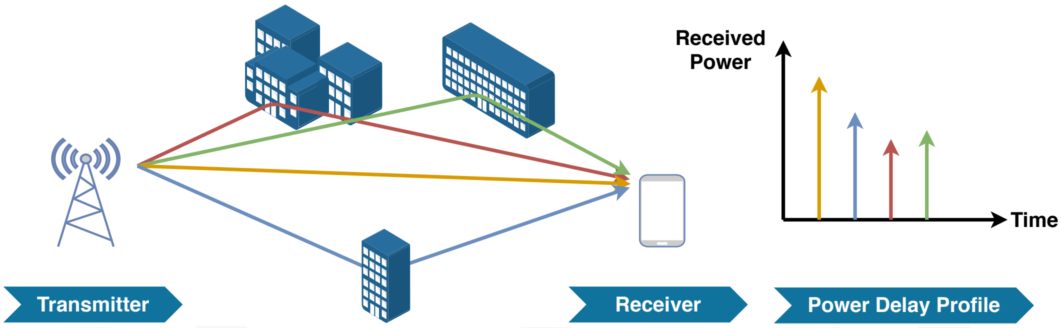

Figure 2.6 : Multipath environment

Just like the effect of Doppler shift on the signal in time, time dispersion causes fluctuations in frequeny domain. As time dispersion increases, constant amplitude bandwidth will decrease in frequency. Constant amplitude bandwidth which is known as *coherence bandwidth* is given in the Formula 2.5.

$$B_c \approx \frac{1}{5\tau_{rms}} \tag{2.5}$$

where τ_{rms} is RMS delay spread. Therefore, the coherence bandwidth is inversely proportional to the effective delay spread.

As a result, if the signal bandwidth is shorter than the coherence bandwidth, flat fading occurs. Similarly, if the signal bandwidth is greater than the coherence bandwidth, frequency selective fading occurs.

Summary table of fading channel characteristics is given in Figure 2.7. Here, T_s is symbol period and B_s is symbol bandwidth.

2.4 Modeling of Fading Channels

In the previous section, the main sources of the problem are mentioned. Researchers work with some models to solve these problems. By building the model, the problem is defined and the best solution can be produced. For instance, some distributions are

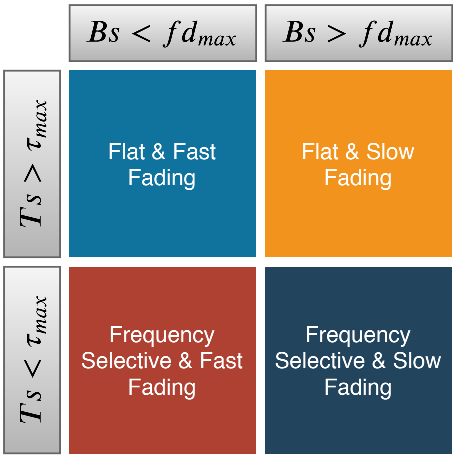

Figure 2.7 : Summary table of fading channel characteristics

observed to adapt to the characteristics of the channel for the amplitude fluctuations. In this section, the most used two amplitude distributions will be examined.

2.4.1 Rayleigh distributed fading

Scattering occurs when an electromagnetic wave hits a surface i.e. multiple copies of the signal scatter around from the objects. According the Central Limit Theorem (CLT), if there are many objects in the wireless communication environment, impulse response of the channel will be well-modeled as a Gaussian process. Further, if there is no Line of Sight (LOS) connection or dominant component to the scatterer, then the process will be zero mean and phase will be uniformly distributed between 0 and 2π. In this case, if the imaginary and real component is Gaussian distributed, the amplitude of the fading coefficient will be Rayleigh distributed.

Probability density function of Rayleigh distribution is given as

$$p_x(x) = \frac{2x}{\Omega} \exp\left(-\frac{x^2}{\Omega}\right), \quad x \geq 0 \tag{2.6}$$

where Ω is the shape parameter. This parameter will be large, if the components have large variances.

As fading coefficient of the channel is distributed according to Rayleigh, corresponding the instantaneous SNR per symbol of the channel γ is distributed according to exponential distribution. Probability density function of corresponding exponential distribution is given as

$$p_\gamma(\gamma) = \frac{1}{\bar{\gamma}} \exp\left(-\frac{\gamma}{\bar{\gamma}}\right), \quad \gamma \geq 0 \tag{2.7}$$

where $\bar{\gamma}$ is the average SNR per symbol.

Probability density function of the Rayleigh distribution with various shape parameter Ω is given in Figure 2.8.

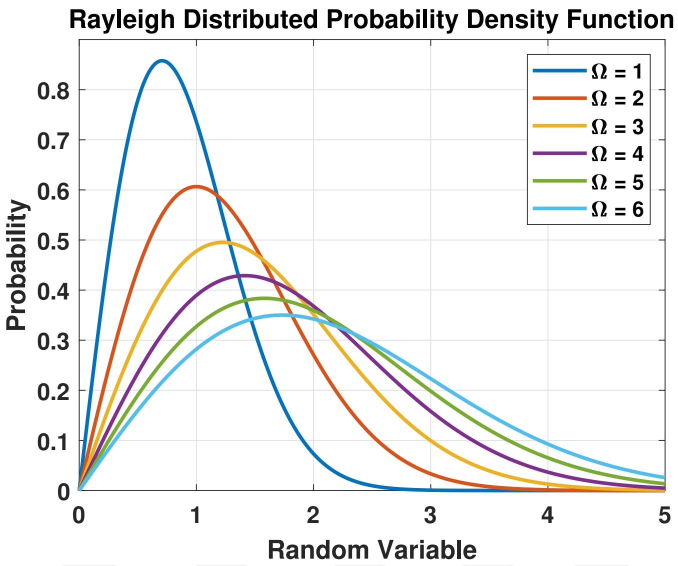

Figure 2.8 : Rayleigh distributed probability density function

2.4.2 Nakagami-m distributed fading

Wireless channel characterization fits Nakagami-m distribution, when there are contributions from both diffused and specular scattered components, i.e., specular component with diffused components have less energy reaches to the receiver.

Probability density function of Nakagami-m distribution is given by

$$p_x(x) = \frac{2m^m x^{2m-1}}{\Omega^m \Gamma(m)} \exp\left(-\frac{mx^2}{\Omega}\right), \quad x \geq 0 \tag{2.8}$$

where Γ is gamma function, m is the Nakagami-m fading parameter (shape parameter), which ranges from $\frac{1}{2}$ to ∞ and Ω is the spread parameter, which takes values greater than 0.

Nakagami-m distribution is a more general definition of Rayleigh distribution, i.e., it defines other distributions according to various parameters. For instance, it converges one-sided Gaussian pdf ($m = \frac{1}{2}$), Rayleigh pdf ($m = 1$) and AWGN channel ($m \longrightarrow \infty$).

As fading coefficient of the channel is distributed according to Nakagami-m, corresponding the instantaneous SNR per symbol of the channel γ is distributed according to gamma distribution. Probability density function of corresponding gamma distribution is given by

$$p_{\gamma}(\gamma) = \frac{m^m \gamma^{m-1}}{\bar{\gamma}^m \Gamma(m)} \exp\left(-\frac{m\gamma}{\bar{\gamma}}\right), \quad \gamma \geq 0 \tag{2.9}$$

where $\bar{\gamma}$ is the average SNR per symbol.

Probability density function of the Nakagami-m distribution with various shape parameter m and spread parameter Ω is given in Figure 2.9.

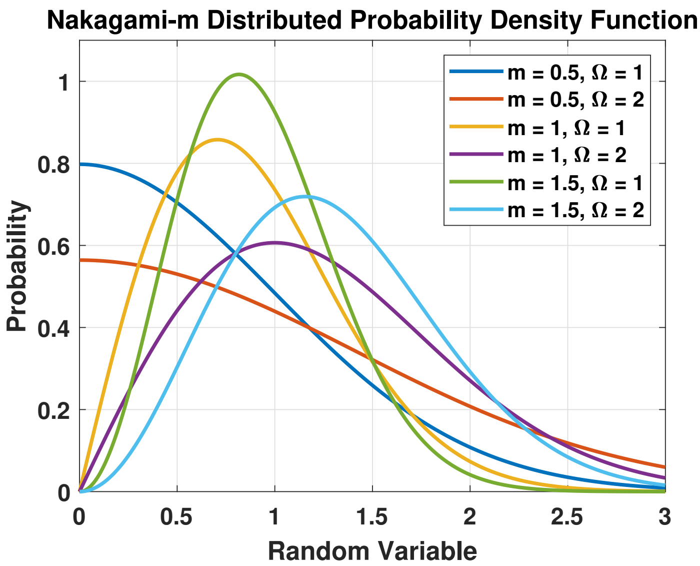

Figure 2.9 : Nakagami-m distributed probability density function

2.5 Maximum Likelihood Detection

In the communication medium, the signal necessarily comes to the receiver with noise. The receiver should be able to detect the information signal from the transmitted signal. Therefore, parameter estimation becomes important. Parameter estimation includes different optimal algorithms for different models. Maximum likelihood estimation provides optimum estimation under certain conditions.

The mathematical model of the received signal is important in terms of decision of detector type and performance. The simple mathematical model of the received signal in AWGN environment is given as

$$y = x + w \tag{2.10}$$

where x is a constant term and w is AWGN noise with zero mean and σ^2 variance. Therefore received signal y is distributed with x mean and σ^2 variance. Joint probability density function of the received signal and transmitted signal is used to estimation of transmitted signal x. Joint PDF is given as

$$f(y;x) = \frac{1}{\sqrt{2\pi\sigma_w^2}} e^{-\frac{(y-x)^2}{2\sigma_w^2}} \tag{2.11}$$

Joint probability density function is a function that gives how the received signal and the transmitted signal changes jointly. It can be found in marginal distributions using this function.

As the noise power increases, the performance of the estimation decreases. This can be intuitively understood with graphics. Joint PDF with noise power $\sigma_w^2 = 0.5$ is illustrated in Figure 2.10 and Joint PDF with noise power $\sigma_w^2 = 2$ is illustrated in Figure 2.11. It can be observed that Joint PDF is more intense on a line with lower variance noise power. As noise power increases, Joint PDF spreads. Consequently, the probability of taking various values of the transmitted signal increases. In this case, the distribution of the received signal also spreads. Therefore, the estimation performance is affected.

From Figure 2.10 and Figure 2.11, it can be seen that the accuracy of the decision-making may change depending on the strength of the noise. In both figures, distributions are depicted on a single sample. In Equation 2.11, the distribution of a single observation is defined. Since the distribution does not only depend on observation, but also to the input, it is also called the *likelihood* function. The highest value that the likelihood function takes is called the *maximum likelihood estimate*. The power of noise affects the reliability of this estimation.

Figure 2.12 depicts the distributions that occurs when two separate observation data are obtained. For instance, since the noise is zero mean and observed data y is -2, the maximum likelihood estimate $\hat{x}$ is -2 according to the resulting distribution. Likewise if the observed data y is 1, the maximum likelihood estimate $\hat{x}$ is 1 according to the resulting distribution.

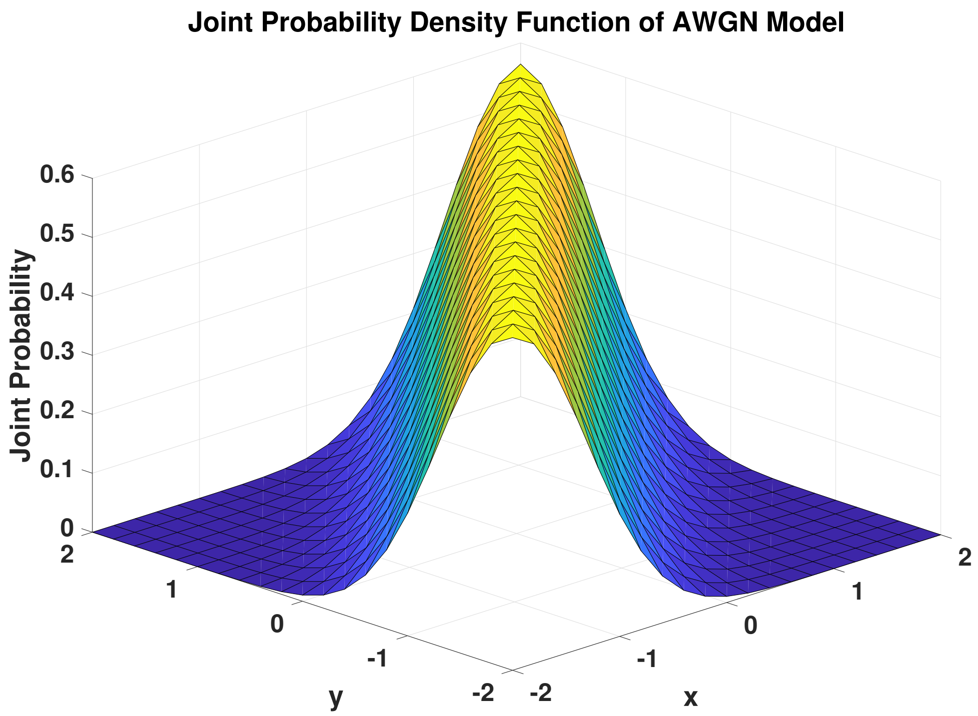

Figure 2.10 : Joint PDF with $\sigma_w^2 = 0.5$

In 2.10, the model is defined for a single observation. As the number of observations increases, the distribution and dimension of Joint PDF will change. The reliability of the obtained estimation with increasing observation data will also change.

Vector representation of the AWGN model is obtained with many observation data. It is a function of the time. It is evaluated the input as constant during the observation period. Vector model of the constant input is given as

$$y(n) = x + w(n) \tag{2.12}$$

Assuming that all observations are independent of other observations in the observation period, resulting Joint PDF is given as

$$f(\mathbf{y};x) = f(y(0);x) * f(y(1);x) * \cdots * f(y(N-1);x) \tag{2.13}$$

The maximum value $\hat{x}$ is the maximum likelihood estimate of the input when $\mathbf{y}$ is observed. Maximizing this function is also equivalent the maximizing of the natural logarithm of this function. Natural logarithm of this function is called as *log-likelihood*

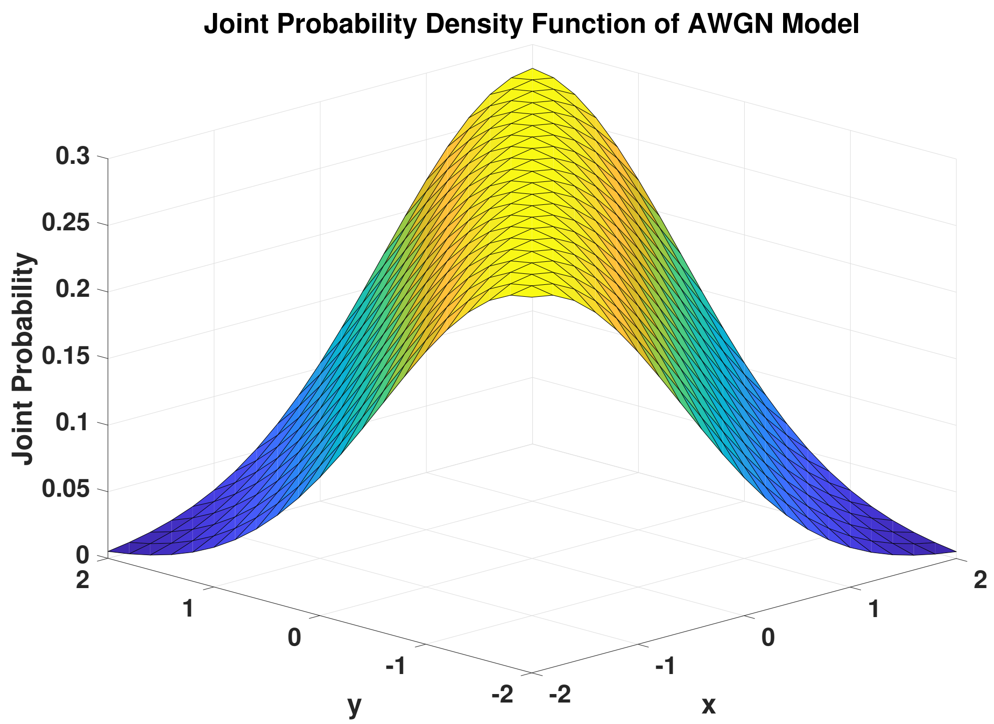

Figure 2.11 : Joint PDF with $\sigma_w^2 = 2$

function. Maximizing log-likelihood function is also equivalent minimizing cost function obtained from derivation of the log-likelihood function and it is given as

$$J(x) = \sum_{n=0}^{N-1} (y(n) - x)^2 \tag{2.14}$$

Therefore, the minimum value of this function is equivalent of the maximum likelihood estimate of the input.

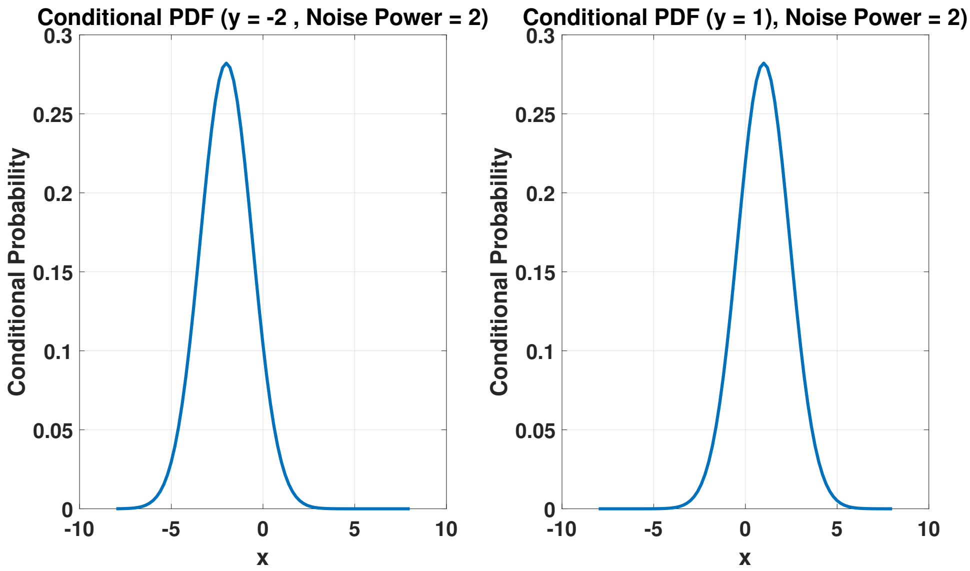

Figure 2.12 : Conditional PDF with various observations

3. A BRIEF INTRODUCTION TO DEEP LEARNING

Classical methods use mathematical models to produce an optimal solution. In contrast, DL methods search for an optimal solution step by step in the training phase. In this section, general concepts of DL are explained briefly and implementation on single carrier systems is described.

3.1 Multilayer Perceptron

Basically, a MLP is a deep, artificial neural network and it is composed of more than one perceptron. An example for MLP is given in Figure 3.1. Typically, the data is fed to the input layer as a vector and therefore, if the input data is two dimensional vector (e.g. image) or high dimensional vector, it must be converted to the vector format to fed the input layer. The data in the input layer is multiplied by weights along each connection and added a bias terms as it passes through neurons of the first layer. After going through a predefined activation function, the output of the neurons are obtained. Then, the output of those neurons are then transmitted to the neurons in the next layer in the same way.

The final layer that the data reaches through the network is the output layer. An estimate of the network is obtained for the desired result in the output layer. A network can perform a classification task or a regression task (or both).

3.1.1 Building model

A neural network model can work linearly to handle linear problems. Nonlinear problems can also be solved by neural networks through the use of activation functions.

Neural networks have ability to solve nonlinear problems with the help of activation functions as mentioned above. Some commonly used activation functions are depicted in Figure 3.2. For instance, sigmoid and ReLu activation functions are two

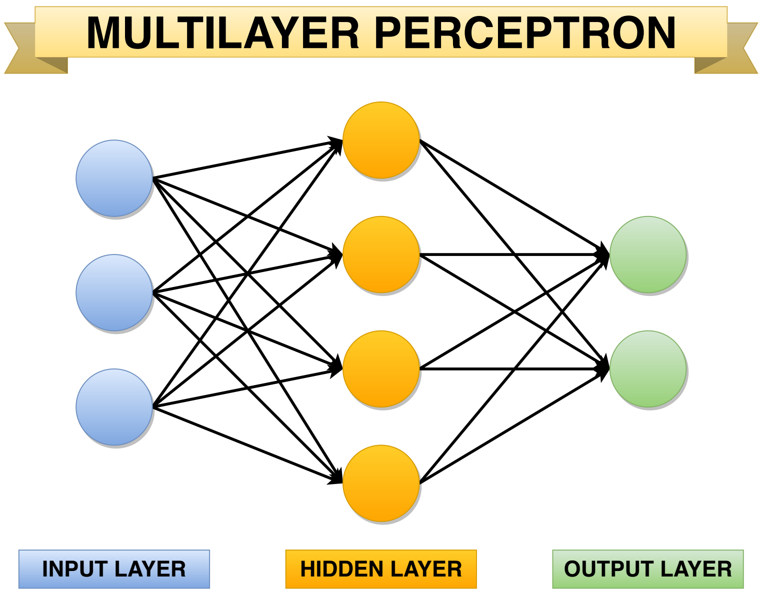

Figure 3.1 : Multilayer perceptron architecture

examples for activation functions and they both can be used in various regression and classification tasks.

The essential building block of a typical neural network is perceptron. A perceptron consists of only one neuron and activation function. It, therefore, produces a single output value (**y**) as follows:

$$y = \phi(\mathbf{W}^T\mathbf{x} + b) \tag{3.1}$$

where y represents the output, $\mathbf{x}$ is an input vector, $\mathbf{W}$ and b denotes the weight matrix and the bias term, respectively. ϕ represents activation function.

A MLP is a neural network containing multiple layers if all the layers are formed of perceptrons. MLPs with one hidden layer are capable of approximating any continuous function. Perceptron can solve only limited and relatively easier problems(e.g. XOR, NOT, AND etc) but thanks to the MLP, computers are no longer limited by XOR cases and can learn richer and more complex models.

3.1.2 Training phase

Training the model with labeled data is called supervised learning. In supervised learning training, the algorithm tries to produce correct output (estimate) using labeled dataset. This estimate is obtained by multiplying input values with several weight

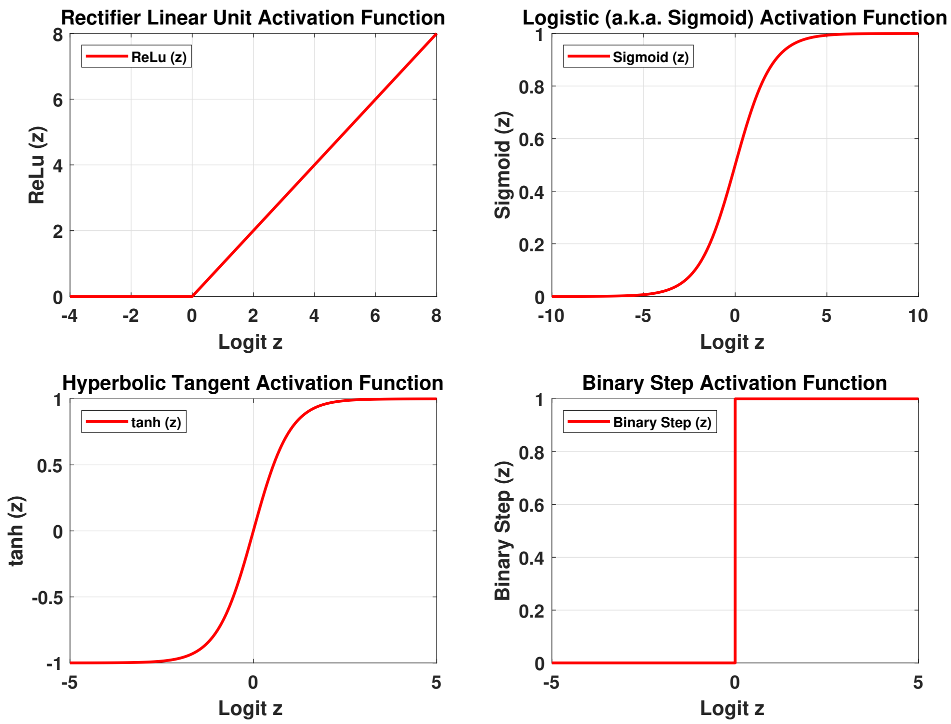

Figure 3.2 : Commonly used activation functions

coefficients and adding several bias terms. Then, the loss function is tried to be reduced by means of an optimizer. Here, the loss function should be selected so that the output of the neural network best suits the labels. For instance, the binary cross-entropy loss function is as follows

$$\mathscr{L}(y,\hat{y}) = -y\log(\hat{y}) - (1-y)\log(1-\hat{y}) \tag{3.2}$$

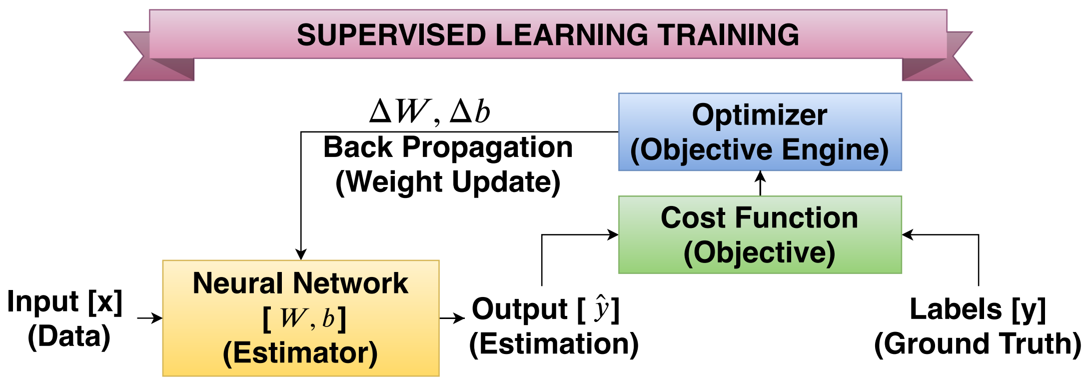

Figure 3.3 : Training phase of supervised learning algorithm

The loss function is chosen to suit the problem so that the neural network can produce a better prediction result and the optimizer can approach the correct result as quickly as possible.

The optimizer acts as an engine running the objective function and its task is to ensure that the loss function reaches the optimum value in the fastest and most accurate way. Since the neural network works step by step, the optimizer moves the neural network weights and bias values in a direction that reduces the loss function at each step. The optimizer's production of weight and bias values to reduce loss function is called *back-propagation*. Therefore, the value obtained from loss function propagates over weights and bias values. Adam, one of the most popular among optimizers, can perform this task quickly and accurately.

Training is completed after the neural network approaches the best value iteratively or after a certain cycle period.

3.1.3 Testing phase

Optimum weights and bias values are obtained during the training phase. During the testing phase, the system is operated with weights and bias values obtained during the training phase. In order for the performance to be high, the relationship obtained from the data used in the testing phase must be related to the data used in the training phase.

Among the various designs, there are evaluation criteria. Consequently, various metrics are used for the performance of the neural network design. For instance, precision, recall, confusion matrix, accuracy, specificity, F1 score, precision-recall or PR curve, ROC curve.

3.2 Convolutional Neural Network

In machine learning, feature extraction must be prepared by the user. Structures where artificial neural network has features such as both feature extraction and classification or regression are called *deep learning*. Therefore, CNN is a DL technique [24] [25]. The CNN structure is shown in Figure 3.4.

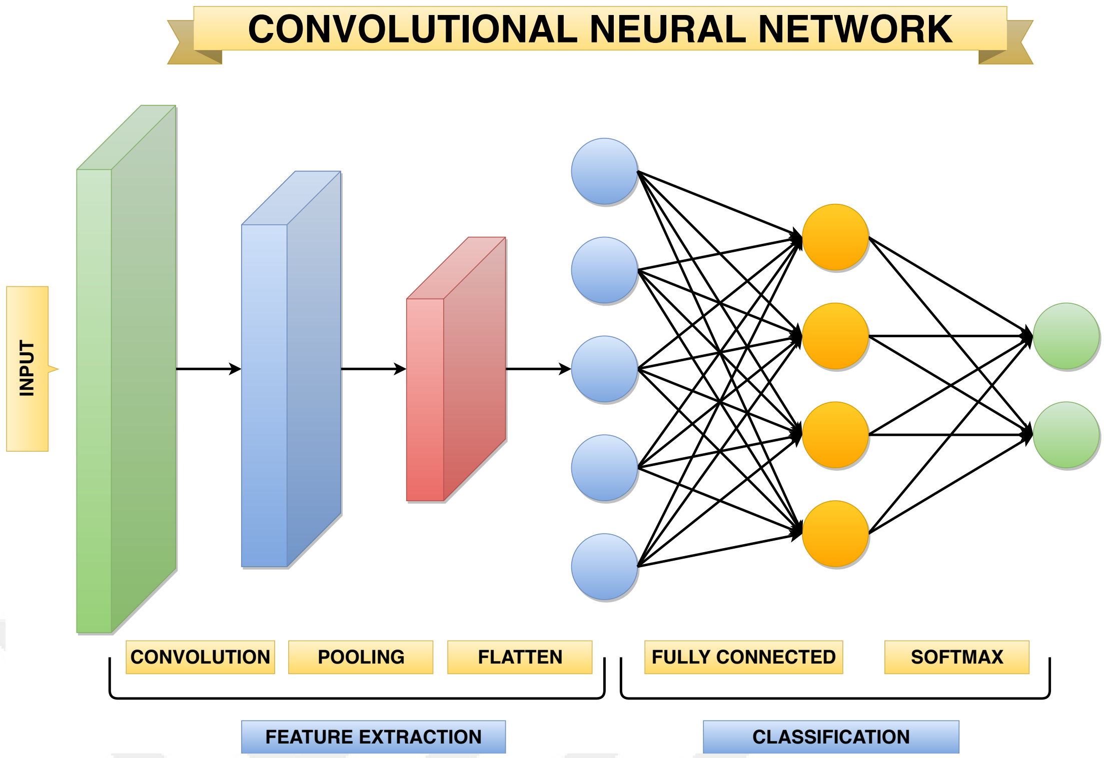

Figure 3.4 : Convolutional neural network architecture

In end-to-end solutions, for example, in classification and regression problems without feature extraction, the data are fed directly to the neural network. For example, when the data is a picture, MLP runs directly on each pixel of the picture.

To classify the data, a CNN uses filters as opposed to MLP. The task of those filters is to extract features by scanning the data. The features obtained becomes input values for the next CNN layer. In the next layer, it is determined whether there is a combination of features in the previous layer. Optionally, this process can be continued with the flattening layer. Consequently, high level features (e.g. edges, motifs for image dataset) are created by combining small level features (e.g. edges-lets, color, gradient orientation for image dataset). In the flattening layer, the data prepared in the convolution layer is made parallel to be transmitted to the classification layers. Finally, the extracted features from the data are classified with MLP the the final layers.

Max-pooling (down-sampling) layers can be used in after convolution layers. In max-pooling layer, instead of transferring all the values obtained from the convolution layer, the maximum value is transferred.

If a model is trained on a lot of training data, it starts to learn noise and incorrect data inputs instead of generalization in our dataset. This phenomenon is called *overfitting*. The dropout layer is used to prevent overfitting.

3.3 Neural Receiver for Single Carrier Transmission over AWGN Channel

In this section, artificial neural network performance is examined on a PSK modulated single carrier system. The results are compared with the linear maximum likelihood receiver.

In single carrier systems, after the information signal is modulated, it is transmitted with a single carrier. In the multipath channel, the signal sent by a single carrier makes high interference to the other symbol. Therefore, these systems have high ISI. For this reason, complex receiver structures are needed. Also, since single carrier broadband signal is used, it cannot cope with frequency dependent noise. However, in cases where the channel is flat, it is preferred due to its simple structure.

On the receiver side, the single carrier information signal is converted from the passband to the baseband. From conventional linear receivers, the ML receiver detects the data according to the criteria previously given in Chapter 2 Equation 2.14. According to ML criterion, it is detected by determining which symbol in the diagram is closest to the received signal.

Dense neural network with a single output is fed with received symbols to evaluate the performance of the nonlinear receiver. The tanh function is used at the output of the neural network. The reason for choosing this function is that its output takes a value between -1 and +1. Loss function between output of the network and labels is chosen as the mean square error (MSE). Adaptive moment estimation (Adam) optimizer is selected to minimize the loss function.

The linear estimator ML maps the received signal to the closest symbol in the constellation diagram and Unit power BPSK modulated symbols are sent with -1 and +1 symbols. Therefore, ML estimator accepts point 0 as threshold for BPSK. For the single carrier BPSK signal, the optimum receiver is the ML receiver because according to this dataset the best thing to do is to divide it in half and make the decision.

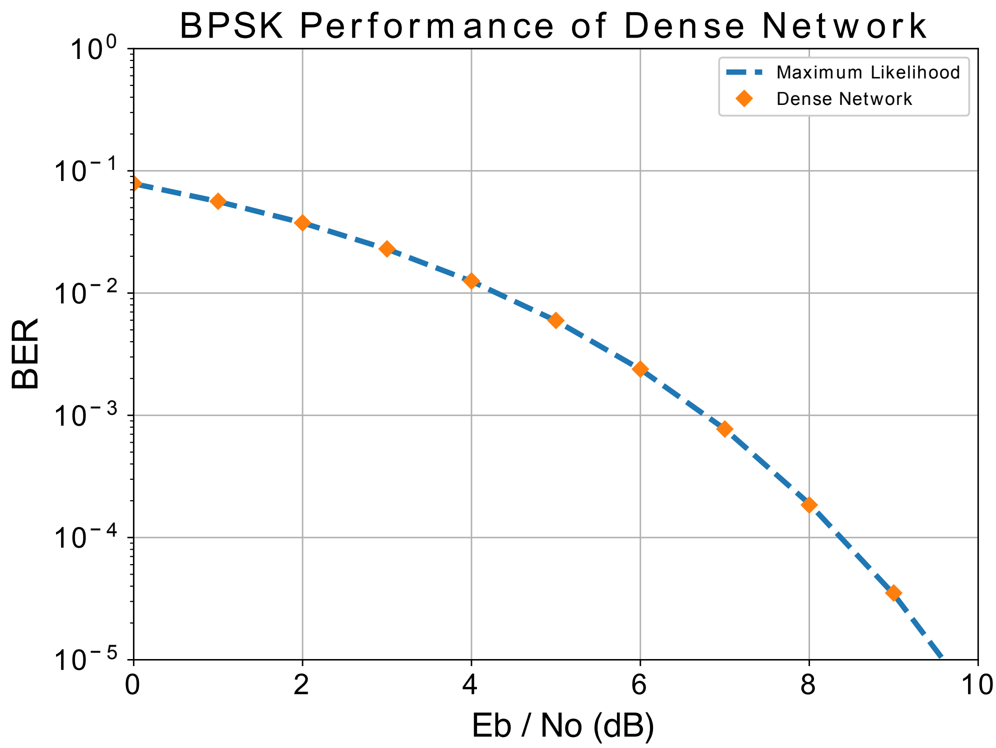

Figure 3.5 : BER performance of dense network for BPSK

In Figure 3.5 dense network performance is shown. The results found match up with BER performance of ML receiver. Figure 3.6 shows the decision threshold of dense network for 14 *dB* SNR. The reason why performance of the dense network is the same as ML is because the decision region is almost the same as the optimum decision region. In Figure 3.7 dense network decision region for QPSK is shown.

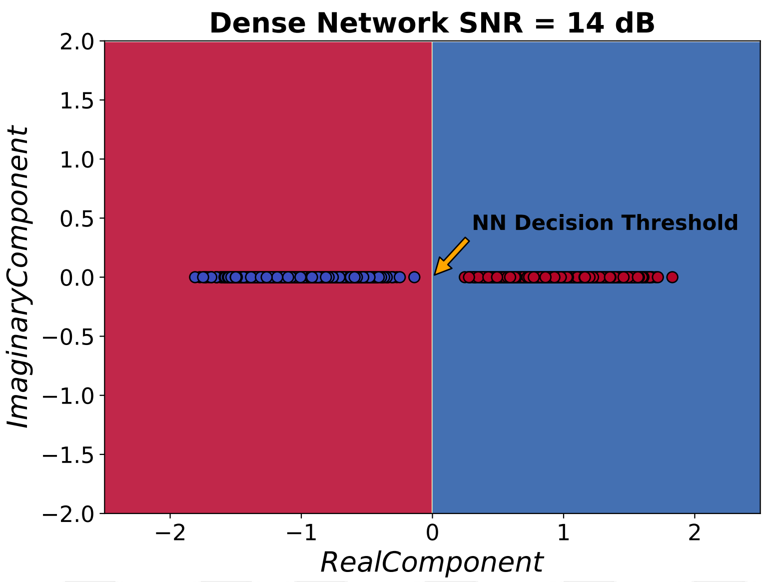

Figure 3.6 : Dense network decision region for BPSK

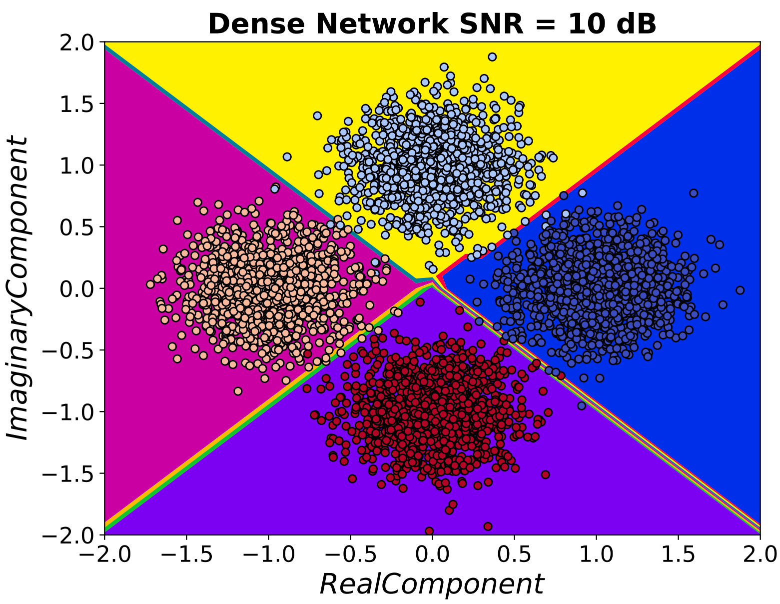

Figure 3.7 : Dense network decision region for QPSK

4. MULTI-CARRIER WAVEFORMS

In this section, classical multi-carrier transmitter and receiver structures will be summarized. Problems and solution approaches will be evaluated. Advantages and disadvantages will be discussed. Classic linear detector structures will also be shown.

Telecommunication is challenging in wireless environments due to the multipath effects which leads to frequency selectivity. Single carrier systems can not cope with this effect due to low symbol period and high ISI. Due to its high bandwidth, it is subject to frequency selectivity. It also has high receiver complexity and bit rate limitation. Multi-carrier systems, on the other hand, convert serial data to parallel data and transmit each through separate subchannels. This makes it possible to extend the symbol duration to achieve the same bit rate. In this way, ISI is reduced. ICI is also reduced by separating the bit stream into subchannels and extending the symbol duration. Thus flexibility in the receiver design is provided.

4.1 Orthogonal Frequency Division Multiplexing

OFDM is a specialized case of MCM method. It was introduced by Chang in 1966 and became popular when it is accepted to form the basic signal format to use within 4G LTE.

OFDM is a frequency division multiplexing scheme and has many usage advantages. It has a lot of subcarriers and each is orthogonal to each other. As a result, inter-carrier interference between the subcarriers is eliminated and intercarrier guard bands are not required. The spectrum efficiency of OFDM is high as the spectra of the subcarriers overlap. It is still separable because of having orthogonal subcarriers. FFT method is used for mapping symbols to subcarriers. The FFT method is a fairly simple method for digital processors. Therefore, it greatly simplifies transmitter and the receiver design and makes digital implementation possible.

Multipath channel is a very important factor that adversely affects performance. OFDM uses cyclic prefix instead of guard time to deal with this effect. Thus, the channel acts circularly instead of linear. After the CP is removed in the receiver and FDE is applied, the frequency selective channel turns into flat fading subchannels. Therefore OFDM can easily adapt to severe channel conditions without complex time-domain equalization and with simple frequency-domain equalization to flat fading subchannels. In addition, OFDM is less sensitive to sample timing offsets and adaptive power allocation to each subbands can be easily implemented.

In addition to the positive aspects of OFDM, there are also some negative aspects. High PAPR occurs because a symbol is a combination of many independent subcarriers. So it requires a linear transmitter circuitry which causes to increase the complexity of ADC and DAC converters. Besides due to cyclic prefix overhead latency is high. Additionally, OFDM is sensitive to doppler shift, carrier frequency offset and phase noise. Due to overlapping subcarrier spectra, high ICI occurs when orthogonality of carriers is lost.

Block diagram of OFDM transmission system is depicted in Figure 4.1. The data produced in the transmitter is first converted into bits and optionally encoded. These bits are divided into parallel bits as many as the number of active payload subcarriers. Parallel bits are mapped according to the desired modulation. The IFFT operation is then performed to the modulated symbols. At this stage, after the samples mapped in the frequency domain have modulated each subcarrier, time domain samples are obtained. Obtained samples are converted from parallel stream to serial stream. To cope with multipath channel effects, a piece is copied from the end of the symbol and pasted to the beginning of the symbol. The resulting OFDM symbol is sent to the receiver through the channel.

On the receiver side, first operation is CP removal. Then the samples are converted to parallel stream. FFT operation is performed to parallel stream. At this stage, the signal is converted from time domain to frequency domain. Channel equalization is carried out by channel coefficients obtained by channel estimation methods. Symbol detection is performed to the equalized signal. Finally, estimated bits are transferred to the bit sink after the symbols are demapped.

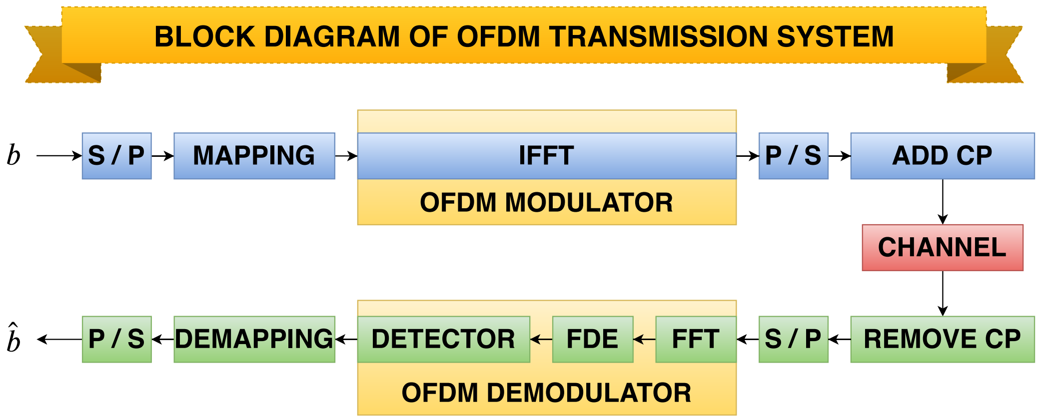

Figure 4.1 : Block diagram of OFDM transmission system

4.2 Single Carrier Frequency Division Multiplexing

In this section, SC-FDM modulation system, which has a single carrier and a close relationship with OFDM, which is a multi carrier system, is examined. Further, it is explained why this system should be evaluated as a multi-carrier system. SC-FDM is used together with OFDM in LTE systems and the reason for this is evaluated.

OFDM transmission system has high PAPR due to IFFT operation. The peak value of the signal consumes high power. Although, mobile devices have limited energy capacity, base stations do not have an energy constraint. Thus, although ofdm is suitable in downlink, it cannot be used in uplink. Therefore, there is a need for SC-FDM transmission systems which has lower PAPR property.

Symbols are mapped on subcarriers with the IFFT operation in the OFDM transmission systems. SC-FDM transmission systems distribute the symbols to all carriers with the FFT-IFFT pair. The critical point here is that the FFT point is smaller than the IFFT point. In this way, the PAPR is reduced. With the FFT-IFFT operation, a single carrier communication system is obtained. Less PAPR can be obtained with high pulse shaping coefficient. While earning in PAPR property, some properties are disadvantageous. Computation complexity increases as more operation are performed on the receiver and transmitter than OFDM. Less data is mapped to the subcarriers and hence the data rate decreases.

In contrast to OFDM, the SC-FDM uses an additional N-point FFT block at transmitter and an N-point IFFT block at receiver. In Figure 4.2, block diagram of SC-FDM transmission system is depicted. The data produced in the transmitter is first converted into bits and optionally encoded. These bits are divided into parallel bits as many as the number of active payload subcarriers. Parallel bits are mapped according to the desired modulation. The M-point FFT operation is then performed to the modulated symbols. This operation spreads the data to M subcarriers. The next operation is that allocation M data to N subcarriers. It gets the name LFDMA by allocating the data of different users to a local region. Likewise, it gets the name IFDMA by allocating the data of different users to a interleaved region. The IFFT operation is then performed to the allocated symbols. At this stage, after the samples mapped in the frequency domain have modulated each subcarrier, time domain samples are obtained. Obtained samples are converted from parallel stream to serial stream. To cope with multipath channel effects, a piece is copied from the end of the symbol and pasted to the beginning of the symbol. If this copied part of the signal is larger than multipath channel taps, the frequency selective channel turns into a flat fading channel. Next step is the sending SC-FDM symbol via RF components to the receiver through the channel.

First CP removal is performed on the receiver side. Then the samples are converted to parallel stream. N-FFT operation is performed to parallel stream. At this stage, the signal is converted from time domain to frequency domain. Channel equalization is carried out by channel coefficients obtained by channel estimation methods. Symbol-spaced equalizer or fractionally-spaced equalizer can be used as channel equalization method. FSE operates at twice the operation range of SSE. If nonlinear receiver is desired, decision-feedback equalization can be selected. After deallocating the symbols, M-point FFT operation is performed. Then, symbol detection is performed to the equalized symbols. Finally, estimated bits are transferred to the bit sink after the symbols are demapped.

4.3 Generalized Frequency Division Multiplexing

It is focused on high data rate and reliable coverage for 4G technology. Capacity enhancement, ultra-high reliability, low latency and massive connectivity were desired for 5G technology. GFDM was proposed to meet these needs for 5G.

Besides the advantages of OFDM transmission system, it has some undesirable features. For example, it has high out-of-band emission due to the pulse shape being

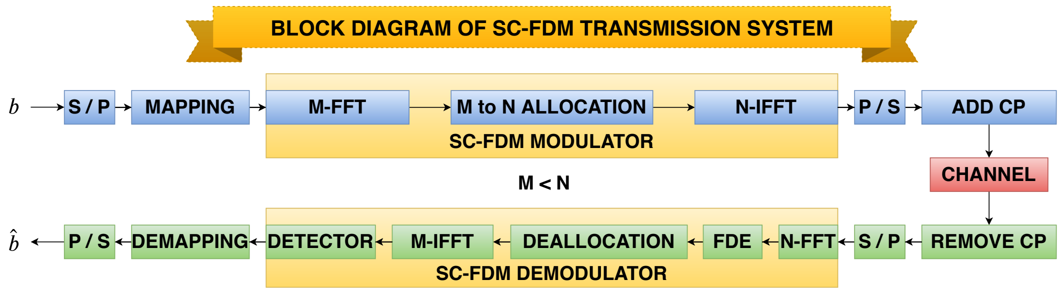

Figure 4.2 : Block diagram of SC-FDM transmission system

square wave. CP is required for each OFDM symbol and hence delay increases. Due to IFFT operation, it has high PAPR. It is very sensitive in terms of carrier frequency shift, which requires advanced synchronization mechanisms to guarantee that the orthogonality does not affect. OFDM is not fully suitable to meet the needs for 5G due to its negative aspects mentioned. In order to achieve the 5G requirements, various multi-carrier based wave-forms are getting considered. GFDM transmission system is one of the considered wave-forms.

The demand of many devices to use the spectrum leads to a scarcity in the spectrum. It is known that OFDM system causes strong spectral leakage even when using pulse shaping techniques or guard channels. Spectral leakage means that the scarce spectrum is not used efficiently. Therefore, GFDM transmission systems are proposed as a solution to this problem. It minimizes leakage in the spectrum with the help of pulse shaping functions. However, pulse shaping functions impair the linearity of the signal. Hence, this leads to ICI and ISI due to the overlapping of the spectrum. Using the pulse shaping function causes increased complexity in the receiver. Various interference cancellation algorithms have been proposed to reduce complexity [26] [27]. By introducing frequency shift offset-QAM technique, implementation complexity and out-of-band radiation in GFDM can be reduced as in [28]. GFDM transmission systems provide the spectral efficiency by removing the requirement of cyclic prefix (CP) for each OFDM symbol with only one cyclic prefix for the entire block.

GFDM falls under the category of filtered multi carrier systems. GFDM is the generalized version of the traditional OFDM and single carrier with SC-FDE. GFDM corresponds to OFDM when the number of subsymbol is equal to 1 and the pulse

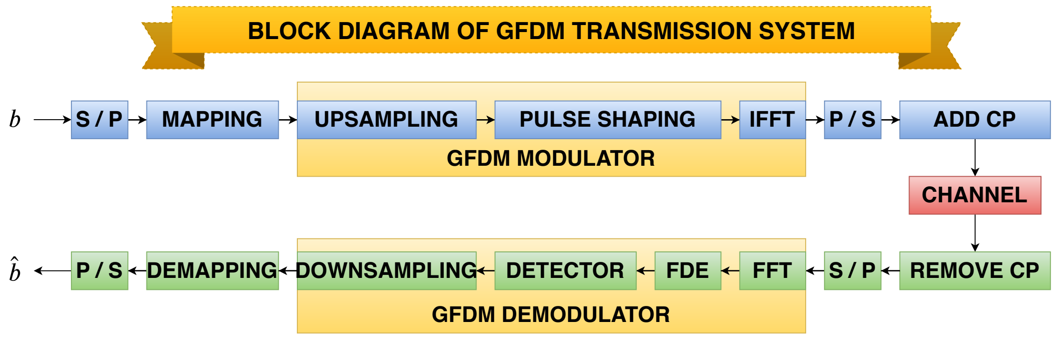

Figure 4.3 : Block diagram of GFDM transmission system

shaping function is square wave. GFDM corresponds to SC-FDE when the number of subcarriers is equal to 1.

In Figure 4.3, block diagram of GFDM transmission system is depicted. The data produced in the transmitter is first converted into bits and optionally encoded. These bits are divided into parallel bits as many as the number of active payload subcarriers. Parallel bits are mapped according to the desired modulation. Upsampling operation is then performed. Next, pulse shaping operation is carried out. According to the type of pulse shaping function, the gain from OOB emission increases, while the loss from ISI and ICI increases. The IFFT operation is then performed to the symbols. At this stage, after the samples mapped in the frequency domain have modulated each subcarrier, time domain samples are obtained. Obtained samples are converted from parallel stream to serial stream. To cope with multipath channel effects, a piece is copied from the end of the symbol and pasted to the beginning of the symbol. The resulting OFDM symbol is sent to the receiver through the channel.

On the receiver side, first operation is CP removal. Then the samples are converted to parallel stream. FFT operation is performed to parallel stream. At this stage, the signal is converted from time domain to frequency domain. Channel equalization is carried out by channel coefficients obtained by channel estimation methods. Symbol detection is performed to the equalized symbols. Next, downsampling operation is carried out. Finally, estimated bits are transferred to the bit sink after the symbols are demapped.

5. DEEP RECEIVER DESIGN FOR MULTI-CARRIER WAVEFORMS

A communication system essentially consists of three parts: Transmitter, channel, receiver. The capabilities of the receiver affects the performance of the communication system significantly. There are three main stages in the receiver design: (I) Antenna design, (II) electronic design and (III) algorithmic design. This chapter focuses on the third stage: algorithm design and studies various strategies to utilize DL in receiver design.

In recent years, as the computing power of computers increase, the use of artificial intelligence also increases in many disciplines. In this chapter, we study the performance of utilizing artificial neural network in the receiver design. A unified multi-carrier system was adopted at the transmitter side. Feature extraction and classification were performed with a deep neural network in an end-to-end fashion. First, the labels were created with the known symbols to obtain the training data, and then, the training was carried out with various deep architectures. The results were evaluated on both OFDM and GFDM-based multi carrier systems. 1D, 2D CNNs and MLP were used as detector network structures and their performances are compared with the performance of various conventional receiver algorithms.

5.1 System Model

In the receiver design, transmitted symbols are estimated with the received signal and available data. While this estimation is made, the effects that the symbol is exposed are modeled. The importance of modeling is that a design can be made to reverse the effects of the symbols is exposed. If the system is modeled, the theoretical performance of the design can also be calculated.

After modeling the system in receiver design, DL based receivers can be used instead of linear receivers for the detection of symbols. In Fig. 5.1 the block diagram of such wireless system is depicted [29]. First, binary data vector **b** is generated by a data source. Coding and 2^{ϕ}-valued complex constellation mapping is performed to

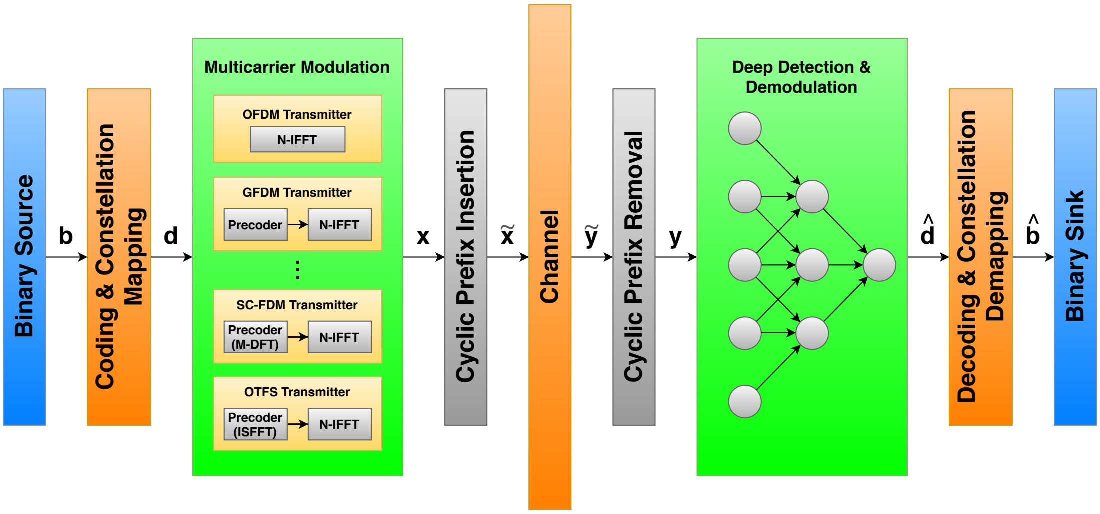

Figure 5.1 : An overview of the proposed deep receiver architecture

obtain symbol vector $\mathbf{d}$, where ϕ is the modulation order. The resulting vector $\mathbf{d}$ has block based structure. Thus, it can be decomposed in frequency and time space into M subsymbols and K subcarriers, wherein K is the total number of subcarriers and M is the number of symbols in one block according to $\mathbf{d} = (\mathbf{d}_0, \ldots, \mathbf{d}_{M-1}^T)^T$ and $\mathbf{d}_m = (\mathbf{d}_{0,m}, \ldots, \mathbf{d}_{K-1,m})^T$. The total number of symbols in one multi-carrier waveform symbol becomes $N = KM$.

N dimensional $\mathbf{x}$ time vector is created by modulating the $\mathbf{d}$ matrix according to the desired multi-carrier waveform type such as OFDM, GFDM, SC-FDM, SC-FDE or OTFS as in Eq. 5.1

$$x(n) = \sum_{k=0}^{K-1} \sum_{m=0}^{M-1} d_{k,m} g_{k,m}(n), \quad n = 0, \ldots, N-1 \tag{5.1}$$

The model of $g_{k,m}(n)$ vector differs according to the desired waveform type. For example, in GFDM, the $g_{k,m}(n)$ is defined as shown in Eq. 5.2; there, operations such as pulse shaping, upsampling and frequency shifting are applied on vector $\mathbf{d}$:

$$g_{k,m}(n) = g\big((n - mK) mod N\big) exp\left(j2\pi \frac{k}{K} n\right) \tag{5.2}$$

where $g_{k,m}(n)$ is formed with the pulse shaping filter $g(n)$. Since all the processes that modulate the symbol to be transmitted are linear, they can be collected in a single matrix. The linear relationship between the vectors **x** and **d** is given in Eq. 5.3, which can be exploited in the implementation:

$$\mathbf{x} = \mathbf{A}\mathbf{d} \tag{5.3}$$

The NxN modulation matrix **A** is created as shown in Eq. 5.4 with $g_{k,m}(n)$ which defines the columns of **A**. The mapped bits in **d** are modulated by the modulation matrix **A**. Here, the modulation matrix is selected according to the chosen modulation type:

$$\mathbf{A} = [g_{0,0}, \ldots, g_{K-1,0}, g_{0,1}, \ldots, g_{K-1,1}, \ldots, g_{K-1,M-1}] \tag{5.4}$$

After the modulation is performed, cyclic prefix is added to the resulting modulated signal to cope with multipath channel effects and adding cyclic prefix yields the time vector $\tilde{\mathbf{x}}$ to be transmitted. The received signal is exposed to a frequency selective Rayleigh fading channel as considered in Eq. 5.5:

$$\tilde{\mathbf{y}} = \tilde{\mathbf{H}}\tilde{\mathbf{x}} + \tilde{\mathbf{w}} \tag{5.5}$$

where, we assume that the channel length is shorter than the CP and perfect synchronization is ensured. After removing the cyclic prefix, Eq. 5.5 can we re-written as in Eq. 5.6:

$$\mathbf{y} = \mathbf{H}\mathbf{x} + \mathbf{w} \tag{5.6}$$

where, **y** is N dimensional and the received matrix **H** is the NxN circular convolution matrix created from the channel impulse response coefficients given by $\mathbf{h} = [h(1), h(2), \ldots, h(N_{ch})]^T$, and **w** is N dimensional additive white Gaussian noise (AWGN) vector. The elements of **h** and **w** follow $\mathscr{CN}(0,1)$ and $\mathscr{CN}(0, \sigma_w^2)$ distributions respectively, where $\mathscr{CN}(\mu, \sigma^2)$ shows the distribution of a circularly symmetric complex Gaussian random variable with mean μ and variance σ^2. Combining Eq. 5.6 and Eq. 5.3 yields to Eq. 5.7 as:

$$\mathbf{y} = \mathbf{HAd} + \mathbf{w} \tag{5.7}$$

After zero forced (ZF) channel equalization we obtain the following equation:

$$\mathbf{z} = \mathbf{H}^{-1}\mathbf{HAd} + \mathbf{H}^{-1}\mathbf{w} \tag{5.8}$$

Linear demodulation of the received symbols can be defined as:

$$\hat{\mathbf{d}} = \mathbf{Bz} \tag{5.9}$$

where $\mathbf{B}$ is *NxN* dimensional receiver matrix. Different types of linear detectors, e.g. zero forced receiver $\mathbf{B_{ZF}} = \mathbf{A}^{-1}$,matched filter (MF) receiver $\mathbf{B_{MF}} = \mathbf{A}^{\dagger}$ and minimum mean square error (MMSE) receiver $\mathbf{B_{MMSE}} = (\mathbf{R_w} + \mathbf{A}^{\dagger}\mathbf{A})^{-1}\mathbf{A}^{\dagger}$ can be used to detect the data symbols from the equalized observation signal, where $\mathbf{R_w}$ denotes the covariance matrix of the noise.

The linear receivers mentioned have their own advantages and disadvantages. Zero forced receiver tries to reduce the effects affecting the symbol to zero. It uses the exposed effects to perform this operation. Therefore, the ZF receiver removes self-interference. However, it enhances noise while removing self-interference. This is mostly because the distorting effects are in reducing direction. Matched filter receiver is optimal for maximizing the signal-to-noise ratio in the presence of additive stochastic noise. It uses the symbol constellation or modulation matrix to perform this operation. Therefore, MF receiver maximizes the SNR while introducing self-interference. This is because it strengthens the sign while strengthening the interference. Minimum mean square error receiver balances self interference and noise and performs the best among these three methods. It uses the symbol constellation or modulation matrix and autocorrelation of the noise simultaneously to perform this operation.

For neural network based detection, the received signal $\mathbf{y}$ is fed as an input to a deep neural network. After the estimated symbol vector $\hat{\mathbf{d}}$ is taken from the output of the deep receiver, decoding and constellation demapping operations are performed. The resulting vector $\mathbf{b}$ is sent to the binary sink.

Modulation matrix performs different operations for each wave-forms. OFDM modulation matrix performs N-point IFFT operation which means frequency shifting. GFDM modulation matrix performs upsampling, pulse shaping and frequency shifting. Furthermore, it has circular structure and because of that, it allows the use of cyclic prefix to make frequency domain equalization possible. The magnitude of the GFDM modulation matrix is depicted in Fig. 5.2.

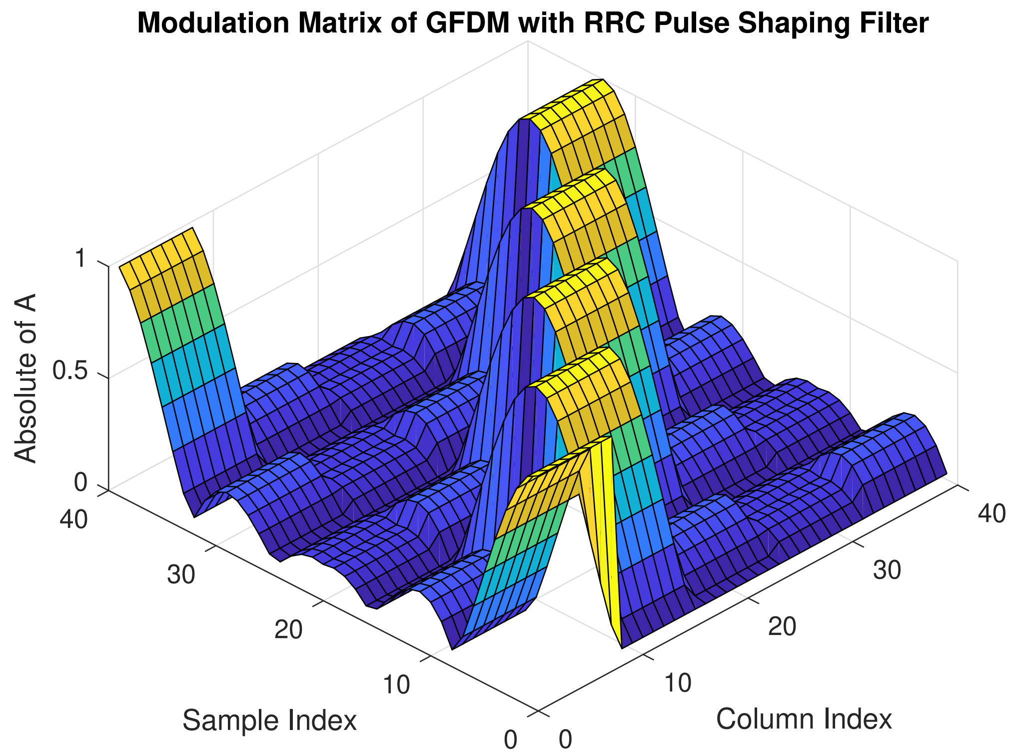

Figure 5.2 : GFDM modulation matrix (K=8, M=5, RRC Filter (a=0.1))

5.2 Deep Learning Aided Receiver Design

Traditional receiver structures used for the unified multi-carrier communication system are mentioned in Section 5.1. These structures decide transmitted symbols according to the solution of the modeled system. If the system works in practice varies according to the modeled system performance in major changes occur. Apart from the algorithms that constantly update the system with prior knowledge, adaptive new solutions cannot be produced. Therefore, there is a need for algorithms that will react instantly to changes in the system. Artificial neural network provides perfect compatibility by updating the solution with training.

Although traditional detection algorithms based on prior knowledge can update, they are not sensitive to changes other than prior knowledge. Hence, it falls short in producing an effective solution. In addition, some prior knowledge cannot be obtained with full accuracy and is estimated. This poses a disadvantage for system success.

In contrast to traditional methods, DL techniques offer a better approach to the solution of the problem. It generates a general solution with the data through the training phase. If a change in system parameters occurs, the artificial neural network shows full sensitivity when a new training is performed and offers new general solution. Therefore, the system renews itself according to the changing parameters. Despite such an advantage, machine learning methods can work with high latency due to training time. In the next sections, transfer learning is mentioned, which reduces the latency of the training phase.

In communication systems, signal detection can be treated as a classification process of recovering the transmitted signal from the (distorted) received signal where a CNN or a MLP can be used for classification in the deep receiver. Therefore, if the symbols to be detected are evaluated as a class, artificial neural network can be used as classifier.

DL techniques provide a general solution without explaining the internal dynamics of the data. In wireless communication, modulation and channel form the internal dynamics of the system. Of these dynamics, the channel has a disruptive effect and must be eliminated. Wireless channel is very variable due to moving objects and multipath channel effects. However, it can be evaluated unchanged at small intervals. If the channel is known in small intervals, the transmitted symbols can be recovered. In classical receiver architecture, pilot signals are often used and the channel is estimated by using those pilot signals. Once the channel is estimated, channel equalization is performed to eliminate multipath effects. The DL technique has the same framework. Deep receiver works in two different modes: Training and Testing. Training mode can be considered as using the pilot signals which can relate to the training data. Using the training data, the model weights are obtained in the neural network to recover the

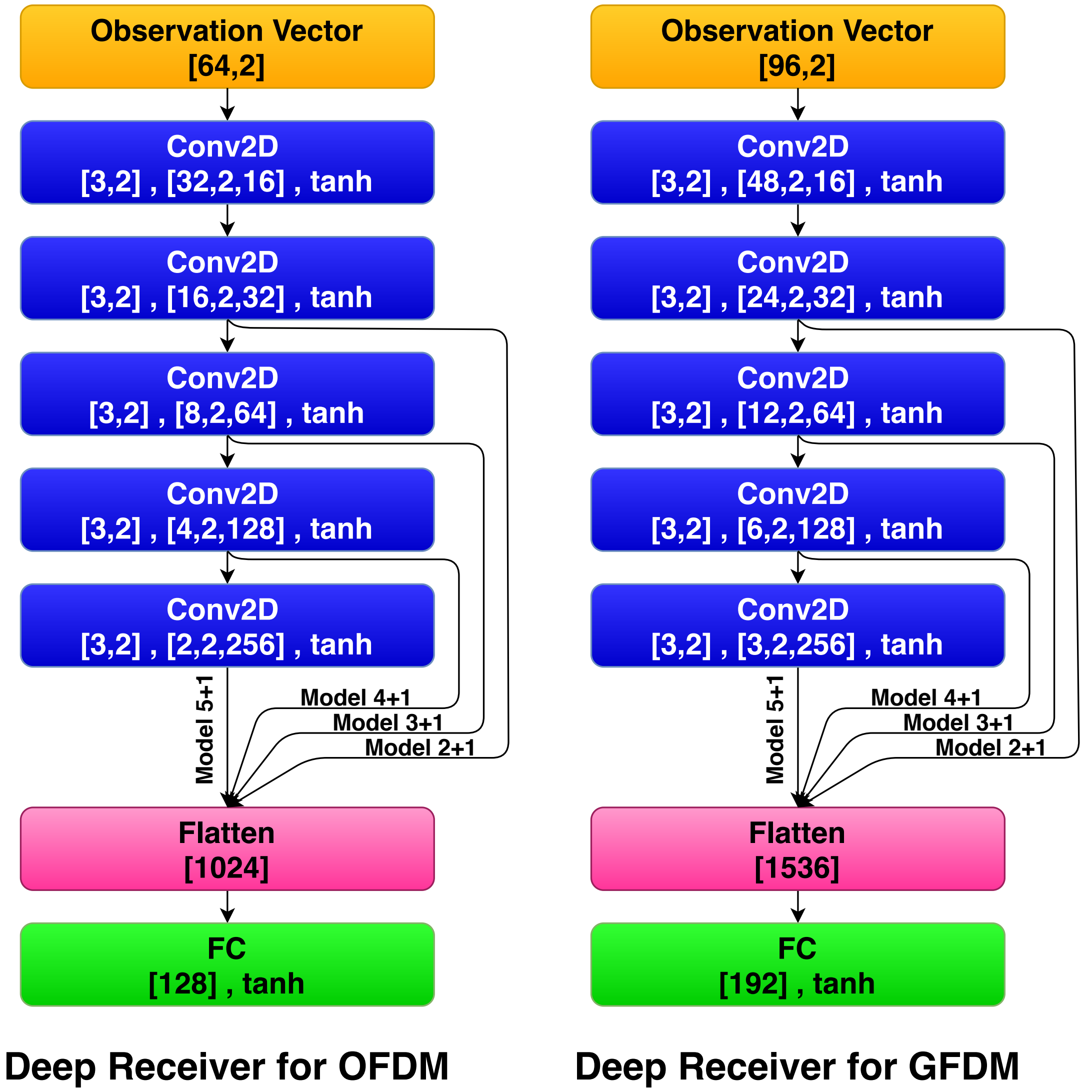

Figure 5.3 : Model Summaries for both OFDM and GFDM

symbols. Testing mode does not require any pilot symbol and works for recovering messages to be wanted to transmit by using weights obtained in the training mode.

MLP, 1D and 2D CNN structures are adopted as the deep demodulation and detection algorithm in Figure 5.1. Network structures are modular designed to be removable and plug-in. MLP receiver consists of 5 different modules. Each module contains layers with different number of neurons (256,128,64,32,16). These modules are then connected to the output layer.

Modular CNN receiver is designed as 1D since the real and imaginary parts of the observation vector are evaluated in series. Likewise it is designed as 2D since the real and imaginary parts of the observation vector are evaluated in parallel. Modular 2D CNN architectures are given in Fig. 5.3 for both OFDM and GFDM. It is used multiple convolutional layers followed by FC layers. Based on the number of used convolutional layers and the number of FC layers, the performance of the deep receiver changes (see Section 5.4). Complex input data is represented as a 2D vector (where each of real and imaginary parts of a complex number forms one dimension). 2D convolution is applied to the input data and deep features are extracted. At the end of the fully connected layers, the symbols are estimated. The vector **d** mapped and coded is used as ground truth while the network is being trained. Adam optimizer is used to train all the networks. Mean Squared Error (MSE) loss function is used in the network during the training as in Eq. 5.10:

$$\mathscr{L} = \frac{1}{N}(\hat{\mathbf{d}} - \mathbf{d})^T(\hat{\mathbf{d}} - \mathbf{d}) \tag{5.10}$$

At the end of the process, it is expected that underlying relationship formed by wireless channel is learned and tried to be eliminated from the signal.

5.3 Transfer Learning

Transfer learning is to use the experience obtained from the previously encountered problem for another problem. In our daily life, people's learning abilities are similar to this concept. An example of this is that it is easier for a person who knows more than one foreign language to learn a new language compared to those who do not speak any foreign language. This is because the person who knows more than one foreign language uses similar structures between languages to learn the new language.

In computer vision field, object recognition, identification and detection is performed in the image. This is done with the capabilities of the convolutional neural network. CNN, which is a DL method, has feature extraction and classification. In convolution layers, low medium and high level features are extracted. This feature can be used in two different neural networks that recognize cats and dogs. For example, in training neural network that recognize the cats, edges, corners and density are determined as a low level feature. Similar low-level features will be needed in the neural network that recognizes the dog. So instead of retraining, these convolution weights are transferred to the other network. The neural network used to detect symbols is mentioned in Section 5.2. During the training, a generalization is made according to the available

Table 5.1 : Simulation Parameters for Both OFDM and GFDM

OFDM & GFDM Parameters used in the Simulations			
Description	***Parameter***	***OFDM Value***	***GFDM Value***
Number of subcarriers	K	64	32
Number of subsymbols	M	1	3
Pulse shaping filter	g	-	RRC
Roll-off factor	a	-	0.1
Length of cyclic prefix	Ncp	16	24
Channel Taps (Fixed)	Nch	10	10

data. When new training data comes in, a generalization is made again. Each process takes approximately 50 to 60 epochs. It was observed that this retraining process took 1 epoch when transfer learning was used. Hence, adaptation is provided very quickly.

5.4 Numerical Results

In this section, the wireless system given in Fig. 5.1 is simulated and studied the performance of the deep receiver for multi-carrier wave-forms. In particular, it is studied the performance for both OFDM and GFDM wave-forms separately. Performance of the deep receiver is compared with the classical methods in terms of bit-error rates (BERs) under various signal-to-noise ratios (SNRs). For comparison, Deep receiver's performance is compared to classical methods including matched receiver with channel equalization, zero forced receiver without channel equalization and MMSE receiver with channel equalization.

5.4.1 Results for OFDM modulation

OFDM parameters selected in the simulations are given in Table 5.1. First 640000 bits are generated to map 10000 OFDM symbols and splitted over 64 subcarriers (K). Cyclic prefix (CP) is inserted at a length of 1 to 4 of the generated time signal. Training data consist of 10000 OFDM symbols and testing data consist of 10000 OFDM symbols. Note that each OFDM symbol carries 64 bits.It is demonstrated how the BER changes with respect to Eb/No (signal to noise ratio) for different configurations. First The performance of a 2D-CNN at different layer numbers (where the total number of convolutional layers varies between 2 and 5) is compared. The results are summarized in Fig. 5.4. In the figure, the best performance is obtained with the 2+1 2D-CNN. It is also demonstrated the performance of another type of CNNs: 1D-CNN. Fig. 5.5 summarizes the results obtained with different 1D-CNNs. The best result is obtained at 2+1 1D-CNN.

Finally, to compare CNN results to MLPs that are formed of only fully connected layers (MLP) it is also studied the performance of multiple MLP networks. The results are shown in Fig. 5.6. The best performance is obtained with 2-layers MLP.

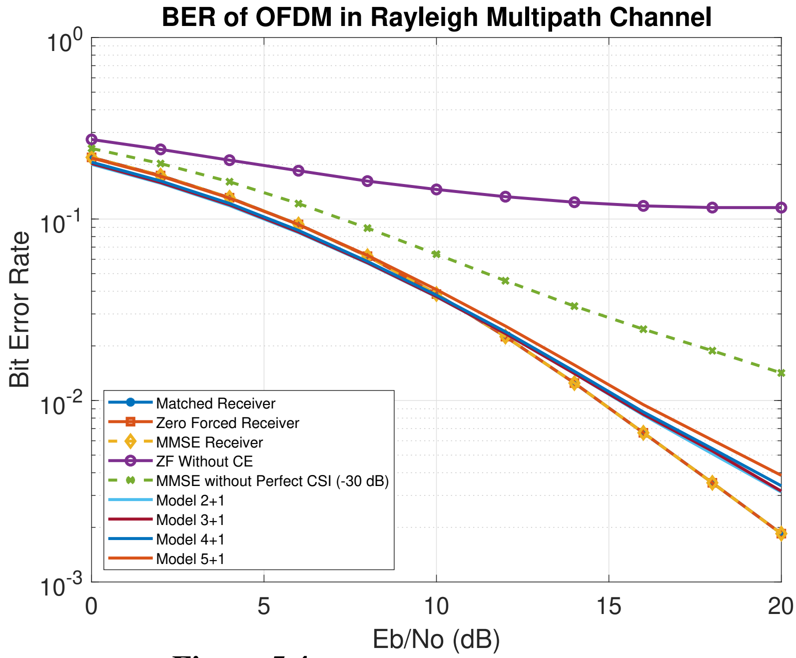

Figure 5.4 : OFDM results for 2D-CNNs

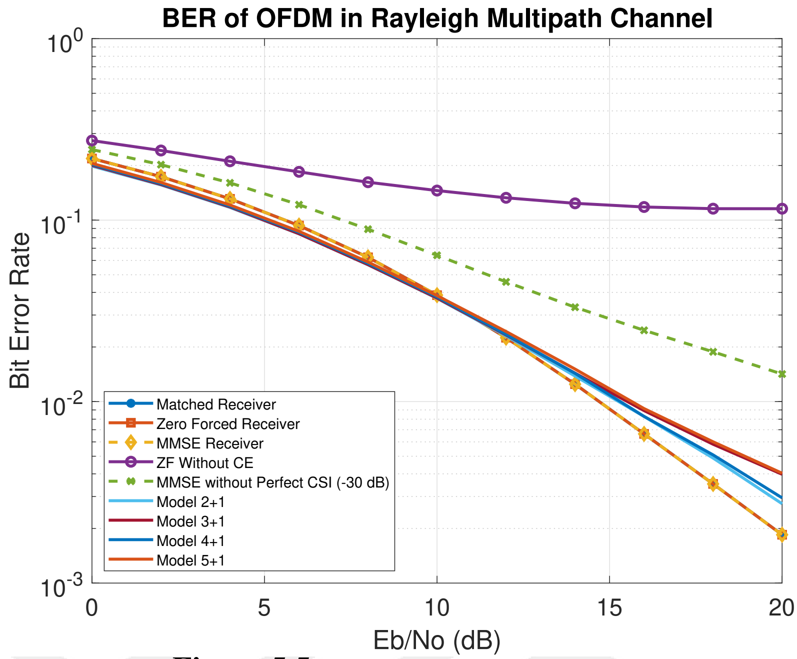

Figure 5.5 : OFDM results for 1D-CNNs

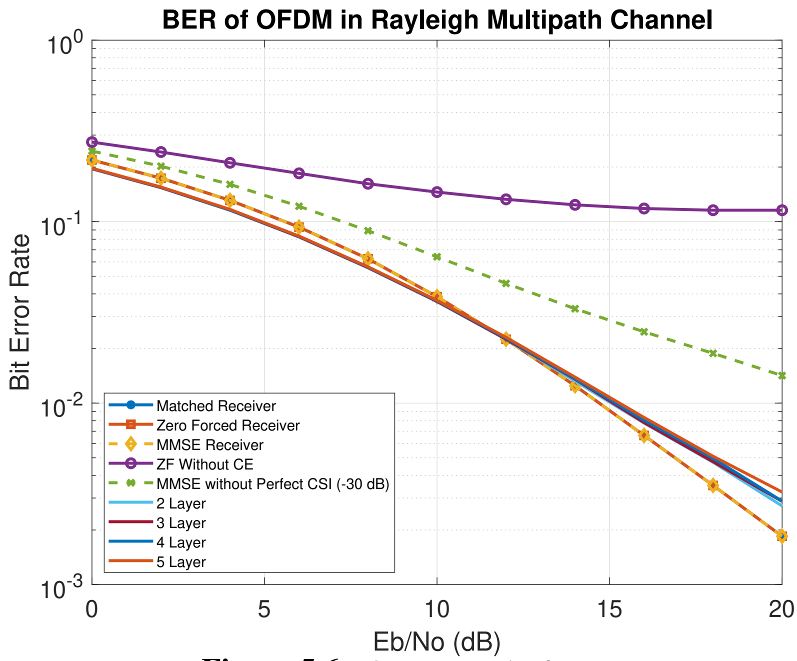

Figure 5.6 : OFDM results for MLP

5.4.2 Results for GFDM modulation

GFDM parameters used in the simulations are given in Table 5.1. First 960000 bits are generated to map 10000 GFDM symbol and splitted over 32 subcarriers (K) and 3 subsymbols (M). These 32 subcarriers and 3 subsymbols located in time-frequency space forms one GFDM symbol. The selected pulse shape for prototype filter of GFDM is the root raised cosine (RRC) filter which is widely used in practice with a roll-off factor (a) of 0.1. Cyclic prefix (CP) is inserted at a length of 1 to 4 of the generated time signal. Training data consist of 10000 GFDM symbols and testing data consist of 10000 GFDM symbols. Note that each GFDM symbols carries 96 bits. In the deep receiver, received complex signal with dimensions of 10000x96 is splitted into real and imaginary parts and a represented as 2D data forming 10000x96x2 dimensional 10000 training symbols. The output dimension is 10000x192x1 real vector. It is demonstrated how the BER changes with respect to Eb/No (signal to noise ratio) for different configurations for GFDM. Similar to OFDM experiments, it is first compared the performance of a 2D-CNN at different layer numbers (where the total number of convolutional layers varies between 2 and 5). The results are summarized in Fig. 5.1. In the figure, the best performance is obtained with the 2+1 2D-CNN. 1D-CNN results are summarized in Fig. 5.8. In the figure, the best result is obtained at 2+1 1D-CNN. The MLP results are shown in Fig. 5.9. In the figure, the best performance is obtained with 2-layers MLP.

In the simulations for both OFDM and GFDM, learning rate of Adam optimizer is set to 0.0001. Dropout layer is added to the output of each layer and we set all the dropout parameter to 0.1 to avoid overfitting.

As can be understood from the simulations, the deep receiver technique provided superiority to the classical receivers. Performance in the theoretical curve for traditional structures is practically unattainable. The reason for this is that the prior knowledge cannot be obtained perfectly. Curve to be reached for -30 dB MMSE receiver in practice is shown with green lines. For the CNN based receiver result, deep receiver methods approach the scenario where the channel is fully known. Note that the deep receiver gives results without channel estimation and equalization. Because the data is given directly to the network without channel equalization. There is also no need for channel estimation, as the known symbols are sent from the transmitter periodically. The network is expected to eliminate the disruptive effects of the channel. In addition, a curve without channel information is given to provide intuition.

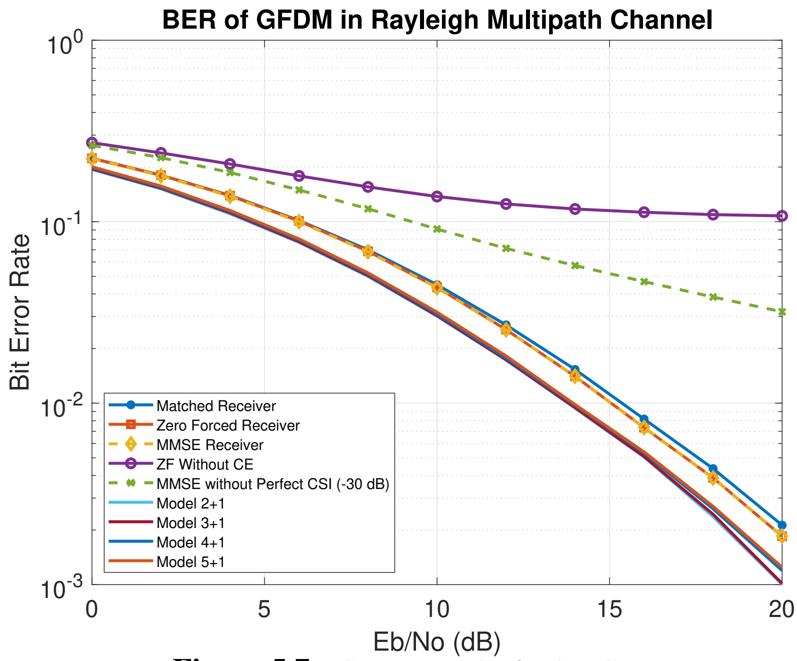

Figure 5.7 : GFDM results for 2D-CNNs

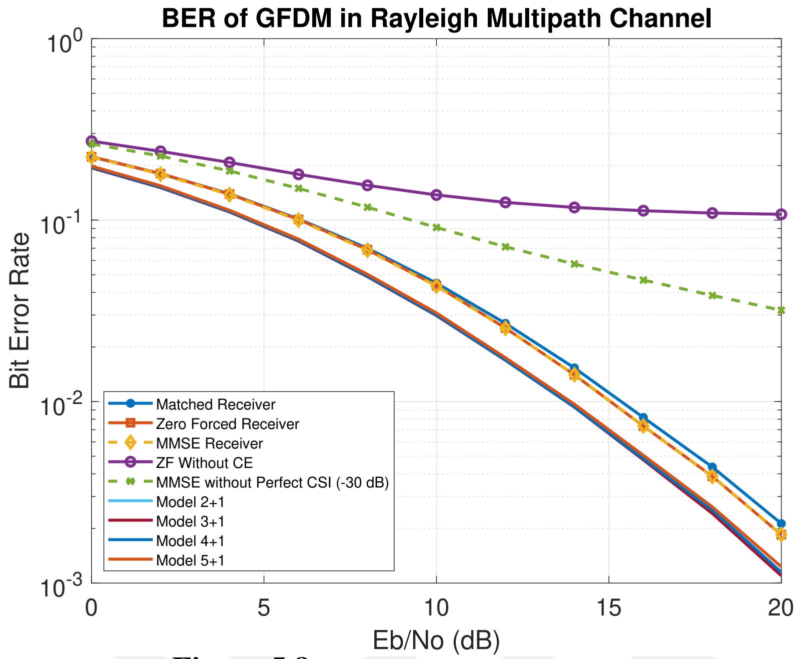

Figure 5.8 : GFDM results for 1D-CNNs

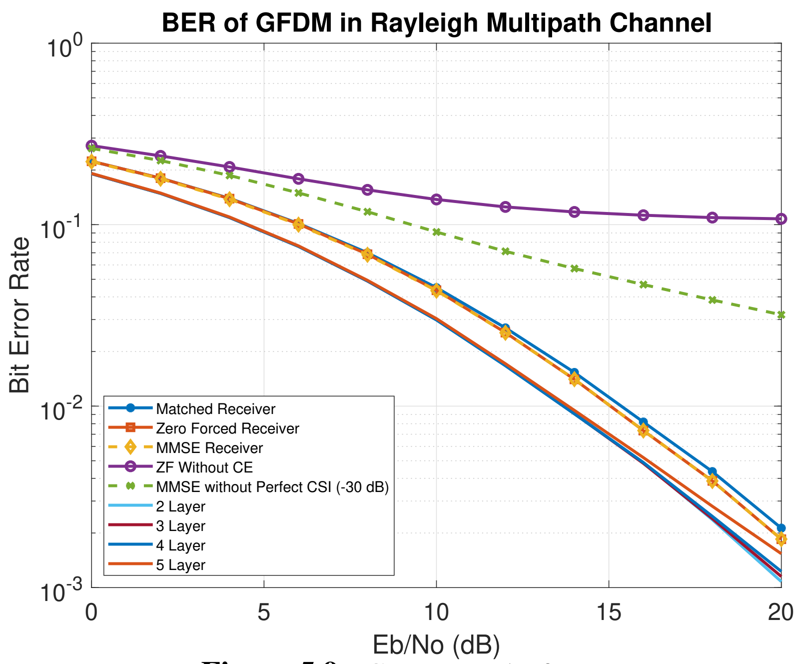

Figure 5.9 : GFDM results for MLP

6. BLIND MAXIMUM DOPPLER SHIFT PARAMETER ESTIMATION

In wireless communication, a disruptive parameter called Doppler effect caused by moving objects negatively affects communication. This effect is examined in Chapter 2. Although the effect affects the wireless channel negatively, the existence of the effect is used in some applications. For example, it is used to measure target speeds on radar, distinguish fixed and moving targets from each other, and measure horizontal range in air or space stationed radar devices, etc.

To eliminate the Doppler frequency effect is possible by stopping all moving objects. This approach is practically not possible. Instead, it would be a realistic approach to estimate the Doppler frequency and spectrum and find solutions to reduce the effect. Doppler estimation was made with transmitted signals, known signals or known prior information in previous studies. This section describes how to estimate the Doppler frequency without the need for any prior knowledge or signal. The estimation consists of SCF, a feature extraction algorithm robust against to AWGN, and an artificial neural network that allows it to measure Doppler frequency.

6.1 System Model

Doppler estimation will be blind as the military scenario is assumed. The signals may be produced from many parameters in the transmitter. Symbols can be produced with different modulation types, parameters, pulse shaping functions, transmitter impurities etc. In addition, the channel disrupts the signal with many parameters during the transfer of information. The degree of freedom is added as much as the parameter affecting the system. Considering that it is desired to obtain information about the channel from the observed signal, the parameter density of the system has a negative impact on the solution of the problem.

Modulated signal consist of message signals and carriers. Message signals are evaluated as random and time varying stationary processes. On the other hand, carrier signals consist of sinusoidal waves and they are completely predictable and deterministic. The final modulated signal is neither stationary nor deterministic, it is evaluated cyclostationary based on the periodicity. Therefore, many predictions can be made using this feature. The signal achieving to the receiver passes through the channel wireless channel. Thus, multipath channel has many effects on modulated signal. This signal can be modeled as in Equation 6.1.

$$r(t) = \Re\{\sum_{n=1}^{N} c_n e^{j\psi_n - j2\pi f_c \tau_n + j2\pi(f_c + f_{D,n})t} .\tilde{s}(t - \tau_n)\} + w(t) \tag{6.1}$$

Here $\tilde{s}(t)$ is the low pass equivalent of the modulated signal generated in the transmitter. This signal, passing through N multipath channels and transmitted at the carrier frequency of f_c, has many effects on the signal when it comes to the receiver. For example, each path has its own characteristic and it effects electromagnetic wave. Attenuation of c_n amplitude occurs on each path. There is also a ψ_n phase change for each path, and τ_n delay occurs, resulting in $2\pi f_c \tau_n$ phase change. Finally, there is a $f_{D,n}$ doppler shift due to objects moving along the path of each wave. Waves passing through this multipath channel overlap in the receiver and subject to additive Gaussian noise.

SCF is calculated by making use of the cyclostationary feature of this signal that comes to the receiver. FAM is preferred among two computationally efficient FAM and SSCA algorithms used in calculating this function. The obtained 2D matrix is given to the artificial neural network and Doppler frequency is predicted by regression.

6.2 Spectral Correlation Function

Estimating the new value in time series is a problem that has been studied for years. While making the estimation process, an estimate is made using the information available. Prediction can only be made if the new value is in a relationship with the past. A better prediction is made if it has more relationships with the past. If it has nothing to do with the previous values, the success of the prediction process will be the same as the random prediction. The relationship of the value to be estimated with the past is determined by autocorrelation. This function, which gives the relationship between two different points, is given as in Equation 6.2.

$$R_x(t_1,t_2) = E\left[x(t_1)\,x^*(t_2)\right] \tag{6.2}$$

To determine how the autocorrelation varies with some particular central time, centralized autocorrelation function is defined as follows

$$R_x(t,\tau) = E\left[x(t+\tau/2)x^*(t-\tau/2)\right] \tag{6.3}$$

Stationarity is one of the most important criteria in predicting. By making use of the stationarity of the signal, it can be predicted about the data to be received or the system parameter in the light of the available information. The autocorrelation function of WSS stationary signals is fixed and does not change over time. Therefore, autocorrelation functions are sufficient to define WSS signals. In some time series there is a cyclical relationship, even if there is no continuous relationship. This means that the mean and autocorrelation functions change periodically with time. If autocorrelation is periodic, this cyclic frequency can be denoted with α and can be expressed in a Fourier series due to its periodic feature as follows

$$R_x(t,\tau) = \sum_{\alpha} R_x^{\alpha}(\tau)e^{i2\pi\alpha t} \tag{6.4}$$

Here, cyclic correlation function found by the fourier transform with integer multiples of fundamental cyclic frequency α is defined as follows

$$R_x^{\alpha}(\tau) = \lim_{T\to\infty}\frac{1}{T}\int_{-T/2}^{T/2} R_x(t,\tau)e^{-i2\pi\alpha t}dt \tag{6.5}$$

If α = 0, cyclic autocorrelation function will be equal to autocorrelation function. Hence, cyclic autocorrelation includes normal autocorrelation. Besides, if the signal is cycloergodic, estimation can be made over the samples.

$$R_x^{\alpha}(\tau) = \lim_{T\to\infty}\frac{1}{T}\int_{-T/2}^{T/2} x(t+\tau/2)x^*(t-\tau/2)e^{-i2\pi\alpha t}dt \tag{6.6}$$

According to Wiener relation, if it is taken Fourier transform of a autocorrelation function, then power spectral density is obtained. Similarly in this case if it is taken

Fourier transform of cyclic autocorrelation function, spectral correlation function is obtained.

$$S_x^{\alpha}(f) = \int_{-\infty}^{\infty} R_x^{\alpha}(\tau) e^{-i2\pi f \tau} d\tau \qquad (6.7)$$

SCF is a very important analysis tool in finding the relationship between spectral components formed at different frequencies as much as α. This feature is particularly powerful in AWGN environments where there is no relationship between spectral components. Therefore, it can be used in variety of signal processing and classification tasks in communications with noise.

6.3 FFT Accumulation Method

Autocorrelation function is not available when calculating the SCF function in the observed signal. Since the autocorrelation function is unknown, an estimate needs to be made. FAM is a temporal smoothing algorithm that predicts SCF. The FAM is a Fourier transform of the cross correlation between the spectral components smoothed over time. With this method, the periodicity of spectral components is determined.

SCF estimation with FAM method is obtained by equation 2.8. In the FAM method, firstly, the operations in Equation 2.9 are applied, and a frequency estimation is made.

$$S_{xy_T}^{\alpha_i + q\Delta\alpha}\left(rL, f_j\right)_{\Delta} = \sum_r X_T\left(rL, f_k\right) Y_T^*\left(rL, f_l\right) g_c(n-r) e^{-i2\pi rq/P} \qquad (6.8)$$

$$X_T(n, f) = \sum_{r=-N'/2}^{N'/2-1} a(r) x(n-r) e^{-i2\pi f(n-r)T_s} \qquad (6.9)$$

Here N is the length of the signal and N' is the subblock length. Sliding length L is generally chosen as $N/4$. $g_c(n)$ is optional data-tapering window with $N * Ts$ duration which is the length of the data block that is processed. $a(r)$ is another data-tapering window with $T = N' * Ts$ duration and P is the number of subblocks. The data is sampled with the sampling frequency of $fs = 1/T$ and cyclic resolution is calculated with $\Delta\alpha = 1/N$. On the other hand, cyclic frequency and spectrum frequency are calculated with $\alpha_i = f_k - f_l$, $f_j = (f_k + f_l)/2$, respectively. Finally n ranges over

N integers. r, k, l ranges over N' integers. In Figure 6.1, the block diagram of SCF estimation by FAM is shown.

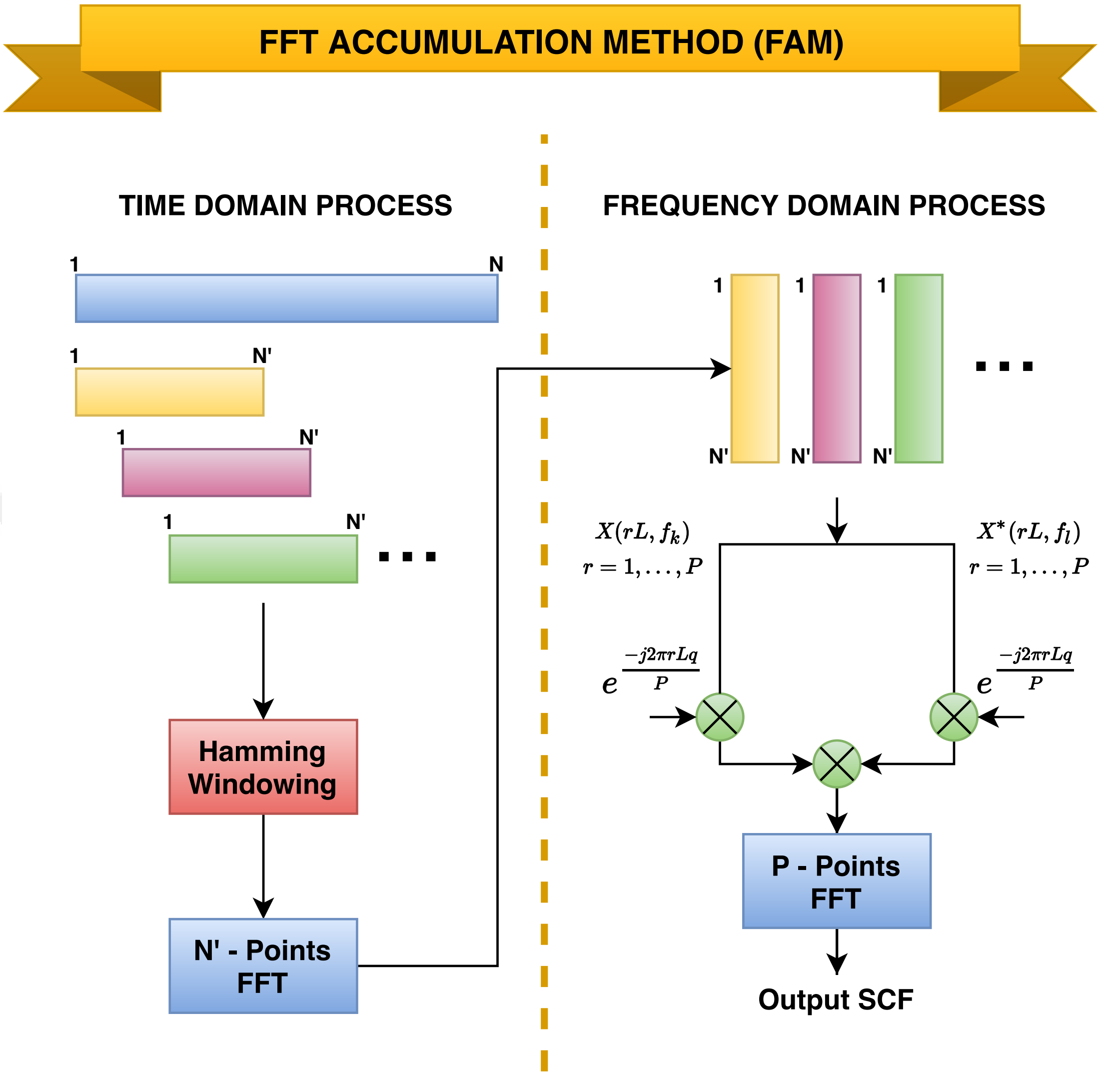

Figure 6.1 : Steps of FAM algorithm

The FAM technique is implemented by input channelization, windowed FFT, down-conversion, multiplication and data reduction and stages is given step by step.

Input Channelization: To make an estimation firstly, the sampled data is divided into P segments of size N' lengths which are intersected each other for spectral estimation. Each segments is saved in a matrix, forming a column. Hence, resulting matrix consist of P column and N' row.

Windowed DFT: Hamming windowing process is applied to all columns separately. Then, the Fast Fourier Transform is performed to all columns. With these processes, the estimation of the spectrum is made from the observation and spectrum of the each windowed segments are separately extracted.

Down Conversion: Calculated spectrum and its conjugate are multiplied with the complex exponential to convert them into baseband.

Pair-wise Multiplication: Pair-wise multiplication matrix is calculated by multiplying the spectrum and its conjugate pairwisely and the results are saved side by side.

Second Windowed DFT and Data Reduction: SCF is calculated by taking Fourier of the pair-wise multiplication matrix. Since this function has no significant data in the first quarter and last quarter, these parts are discarded. Finally the resulting matrix is transferred to the cyclic spectrum domain.

6.4 Blind Doppler Estimation Algorithm

The Doppler effect results from the moving objects in the channel, the receiver and / or transmitter being mobile. Doppler effect causes great distortion in the signal. It is important to measure the amount of this effect. There are some approaches that estimate this effect over the known signals. However, when communicating from point to point, information about the communication system at a third observation point is limited. Therefore, the estimation should be done in blind.

Many parameters originating from the transmitter and the channel are effective on the signal reaching the receiver from the transmitter. The structure to be used to estimate the Doppler frequency should work independently of these parameters or as insensitive to these effects as possible. It should also show similar performances at different SNR levels. For such a system rich in parameter density, making predictions with first-degree statistics is insufficient. Instead, it is focused of high-degree statistics. Of the algorithms used in two different domains in time and frequency, the ones used in the frequency domain are more robust to AWGN. Therefore, algorithms performing on time domain can not be preferred. Also, the signals used in the telecommunication system which are mostly digitally modulated signals exhibit periodicities of statistical parameters. These cyclostationary properties, called spectral correlation features, can be extracted by SCF.

The propagation in the frequency domain and the cyclic frequency domain with the Doppler effect is correlated with the maximum Doppler shift. The Doppler shift acts on the frequencies next to it, so each frequency becomes correlated with the frequencies next to it. This effect of the channel is defined as spectral broadening and results in the spread of SCF in frequency and cyclic frequency. In Figure 6.2, it can be seen as a result of the spectral correlation function of an FM modulated signal exposed to 30 Hz Doppler shift with Gaussian spectrum. In Figure 6.3, it can be seen as a result of the spectral correlation function of an FM modulated signal exposed to 300 Hz Doppler shift with Gaussian spectrum. As it can be seen from the figures, the SCF, which is a high dimensional matrix, has a different distribution according to the severity of the Doppler effect. The variation of the distribution contains information about the maximum Doppler shift. By measuring the amount of spectral broadening, the strength of the Doppler frequency can be estimated. The estimation of the maximum Doppler shift becomes a nonlinear regression problem at this step. Nonlinear regression can be done using one of the DL models, CNNs. CNN is a structure commonly used in computer vision and used frequently in the literature in object recognition, classification, segmentation and regression problems. The output of SCF obtained with FAM is suitable for CNN since it is a 2-dimensional data series. Accordingly, a nonlinear regression model was designed using CNN to estimate the maximum Doppler shift. Linear regression is a linear approach to model the relationship between a scalar system response and one or more descriptive variables. In general, a more advanced regression model should be used when the relationship between inputs and outputs can not be modeled linearly. For this reason, it was evaluated to make nonlinear regression estimation.

In Figure 6.4, Regression CNN designed for Doppler estimation is seen. The matrix produced at the output of the SCF is given as an input to the neural network. There are 4 Convolution layers in the neural network and the features are extracted in these layers. There is a single output FC layer at the end of the network. Huber loss was chosen as the Loss function and the function is as in Equation 6.10. The Huber loss function is a linear function when the error is greater than a certain value, and a quadratic function if the error is small.

$$L_\delta(y, f(x)) = \begin{cases} \frac{1}{2}(y - f(x))^2 & \text{for } |y - f(x)| \leq \delta \\ \delta|y - f(x)| - \frac{1}{2}\delta^2 & \text{otherwise} \end{cases} \tag{6.10}$$

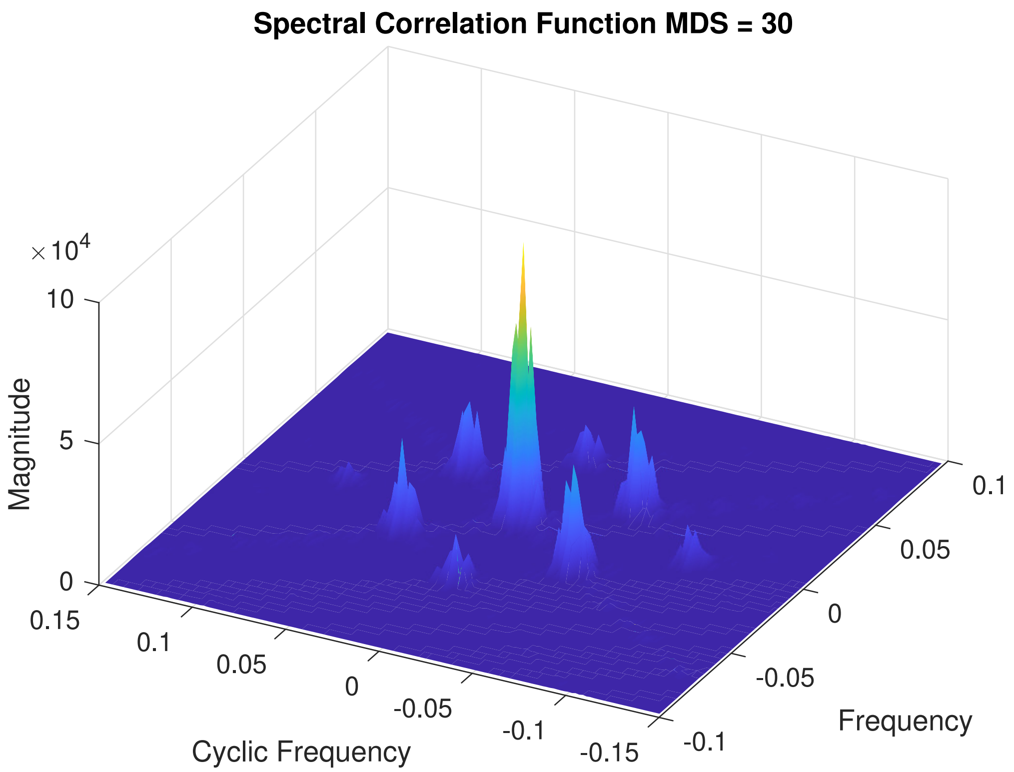

Figure 6.2 : Spectral Correlation Function (FM, Rayleigh, MDS = 30)

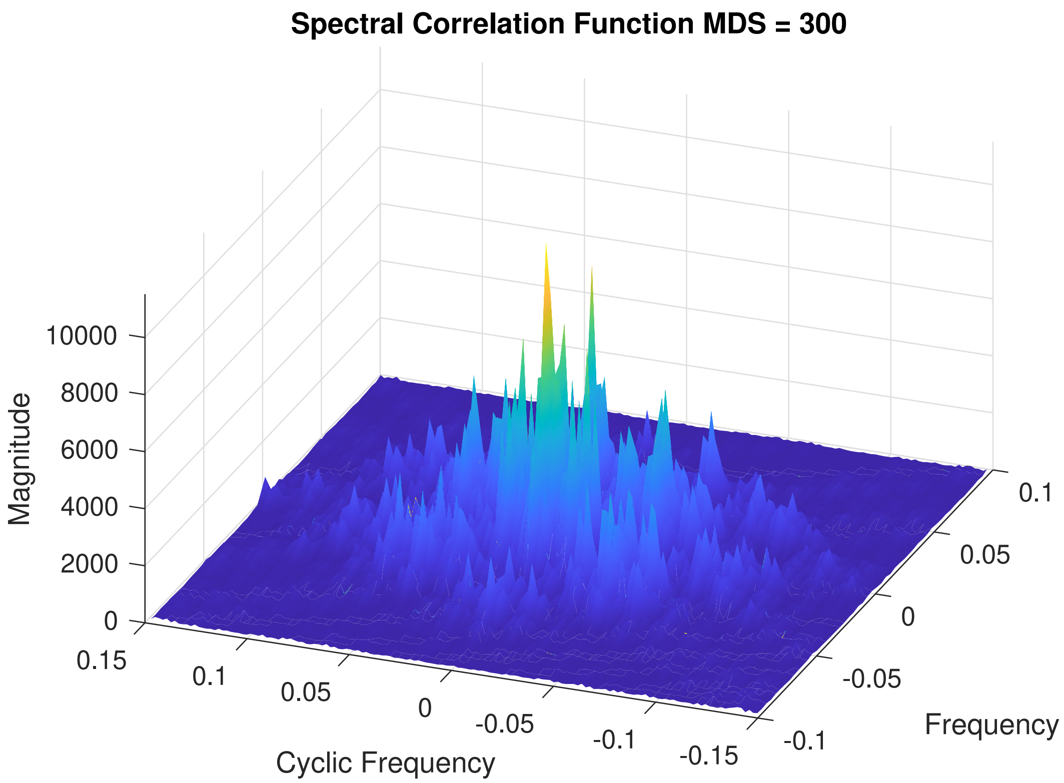

Figure 6.3 : Spectral Correlation Function (FM, Rayleigh, MDS = 300)

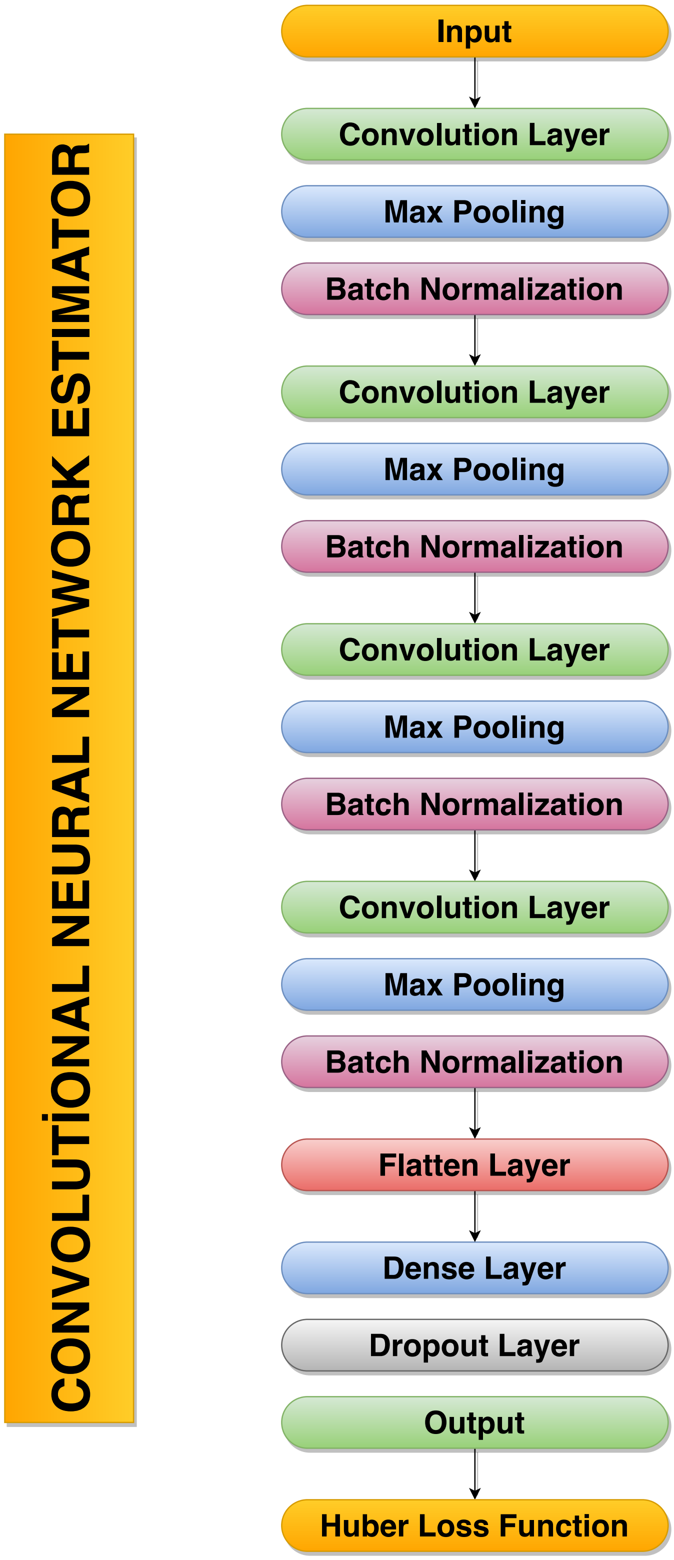

Figure 6.4 : Regression CNN for Doppler estimation

6.5 Numerical Results

In this section, maximum Doppler shift estimation using a nonlinear regression CNN is simulated and performance result is shown. The dataset prepared for estimation includes analog modulation (e.g. DSB-AM, FM, PM and LSB-AM). For each modulation type, modulated signals with SNR values between $-5\ dB$ and $20\ dB$ were produced. Then, these signals were passed through Rayleigh channel and exposed to multipath channel effects and Doppler effects with Gaussian spectrum. The parameters of the channel were chosen randomly and the maximum Doppler shift parameter was stored for the training of the regression model. In the data set Doppler frequency ranges from 1 to 1000 Hz. The generated data set consists of 30000 samples of 10000 lengths. SCF function is calculated with the FAM method with the generated data set. Sampling rate $f_s = 10000$ is chosen. Also, desired frequency resolution and desired cyclic frequency resolution for FAM are selected as $\Delta f = 50$ and $\Delta\alpha = 2$, respectively. After the SCF was estimated from the samples in the data set, dimension of the output become $30000x257x1025$. This 2D data is fed to the input of the CNN Regression network. In Table 6.1, it is given network structure and its parameters that measure the severity of the Doppler effect. The network has 4 convolution layers. Scaled exponential linear unit activation function is used at the output of each convolution layer. The output has a fully connected layer with ReLu activation function. Inputs are given to the network in batch of 32 samples in each step. Adam is used as the optimizer. The training is carried out for 20 epochs. The learning rate is chosen as $lr = 0.00002$.

The results obtained are shown in Figure 6.5. The range of the estimation error is shown with its maximum and minimum points which corresponding mean absolute error. Maximum Doppler shift estimation is made in all analog modulation with an error of approximately 35 Hz at -5 db SNR and 10 Hz at 20 dB SNR. It appears that as SNR increases, performance increases.

Table 6.1 : Neural network structure table for Doppler estimation

Layer	Input	Output	Kernel Size	Number of Kernel	Stride	Activation
Convolution	257x1025x1	257x513x64	7x7	64	[1 2]	SeLu
Batch Norm.	257x513x64	257x513x64	-	-	-	-
Max Pooling	257x513x64	128x256x64	-	-	[2 2]	-
Convolution	128x256x64	128x128x128	3x3	128	[1 2]	SeLu
Batch Norm.	128x128x128	128x128x128	-	-	-	-
Max Pooling	128x128x128	64x64x128	-	-	[2 2]	-
Convolution	64x64x128	32x32x256	3x3	256	[2 2]	SeLu
Batch Norm.	32x32x256	32x32x256	-	-	-	-
Max Pooling	32x32x256	16x16x256	-	-	[2 2]	-
Convolution	16x16x256	8x8x512	3x3	512	[2 2]	SeLu
Batch Norm.	8x8x512	8x8x512	-	-	-	-
Max Pooling	8x8x512	4x4x512	-	-	[2 2]	-
Dense	8192	1024	-	-	-	SeLu
Dropout	1024	1024	-	-	-	-
Dense	1024	1	-	-	-	ReLu

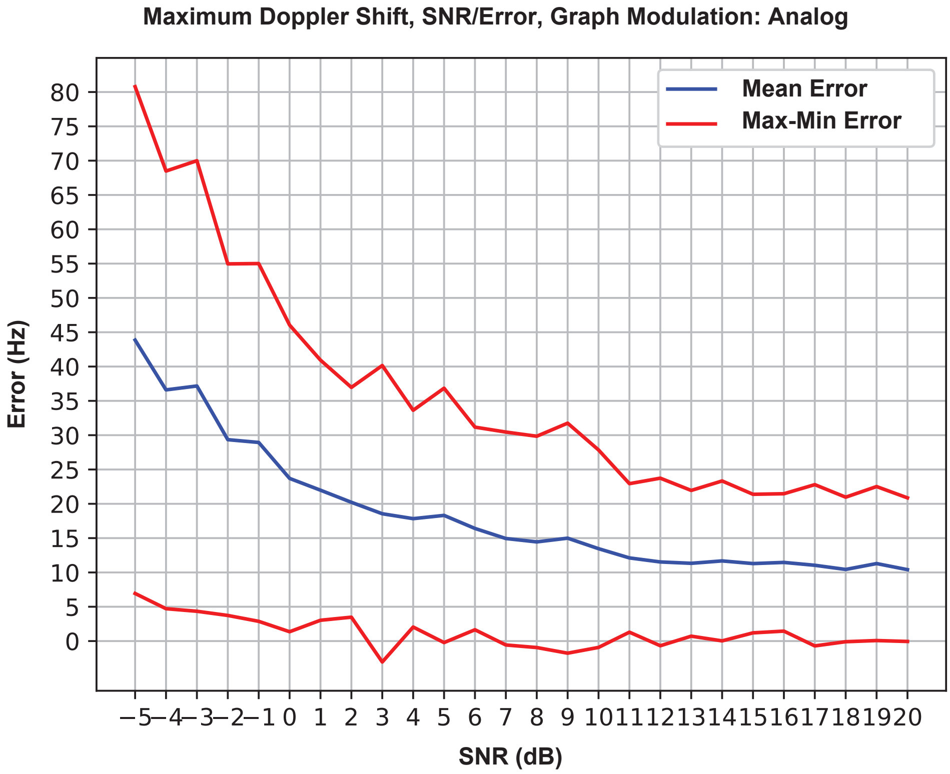

Figure 6.5 : Performance of blind Doppler estimation algorithm

7. CONCLUSIONS AND RECOMMENDATIONS

In this thesis, a deep receiver architecture is presented for multi-carrier wireless systems and blind Doppler shift parameter estimation algorithm. To our best knowledge, this is the first work that introduces data detector without channel equalization using only a deep 2D CNN architecture by eliminating the need for using a coarse detector for multi-carrier systems comparing both OFDM and GFDM. Also this is the first work that estimates maximum Doppler frequency without any prior knowledge.

In our deep receiver, the performance of various neural network architectures including 1D-CNNs, 2D-CNNs and MLPs is analyzed. Furthermore, their performance is compared to the classical techniques. In our preliminary simulations, we studied the performance of different architectures containing different layer types with different hyper-parameters and as shown in our experiments, shallow networks yielded the best performance (while the difference was not much different, when compared to the deeper architectures). For example, for both OFDM and GFDM experiments, 2+1 networks yielded the best BER among CNN architectures. While MLPs can yield slightly better performance for OFDM, they may require significantly more parameters to be kept in the memory.

For blind maximum Doppler estimation, feature extraction was made by using the statistics of the signal with the SCF function. The SCF function was observed to be robust against AWGN noise and also insensitive to all other effects of the channel. Features from the output of SCF function were fed into the regression CNN network, and the strength of the maximum Doppler frequency was measured, and the results were shown. A further study can focus on considering prior knowledge to improve the performance.

REFERENCES

[1] **Chang, R.W.** (1966). Synthesis of band-limited orthogonal signals for multichannel data transmission, *Bell System Technical Journal*, *45*(10), 1775–1796.

[2] **Fettweis, G.**, **Krondorf, M. and Bittner, S.** (2009). GFDM-generalized frequency division multiplexing, *VTC Spring 2009-IEEE 69th Vehicular Technology Conference*, IEEE, pp.1–4.

[3] **Schaich, F. and Wild, T.** (2014). Waveform contenders for 5G—OFDM vs. FBMC vs. UFMC, *2014 6th international symposium on communications, control and signal processing (ISCCSP)*, IEEE, pp.457–460.

[4] **Turhan, M.**, **Öztürk, E. and Çırpan, H.A.** (2019). Deep Convolutional Learning-Aided Detector for Generalized Frequency Division Multiplexing with Index Modulation, *2019 IEEE 30th Annual International Symposium on Personal, Indoor and Mobile Radio Communications (PIMRC)*, IEEE, pp.1–6.

[5] **Van Luong, T.**, **Ko, Y.**, **Vien, N.A.**, **Nguyen, D.H. and Matthaiou, M.** (2019). Deep Learning-Based Detector for OFDM-IM, *IEEE Wireless Communications Letters*.

[6] **Kislal, A.O.** (2018). A Survey on Candidate Waveforms for 5G: Which One Has the Edge?, *Technical Report*.

[7] **Dörner, S.**, **Cammerer, S.**, **Hoydis, J. and ten Brink, S.** (2017). Deep learning based communication over the air, *IEEE Journal of Selected Topics in Signal Processing*, *12*(1), 132–143.

[8] **Ye, H.**, **Li, G.Y. and Juang, B.H.** (2017). Power of deep learning for channel estimation and signal detection in OFDM systems, *IEEE Wireless Communications Letters*, *7*(1), 114–117.

[9] **He, H.**, **Wen, C.K.**, **Jin, S. and Li, G.Y.** (2018). A model-driven deep learning network for MIMO detection, *2018 IEEE Global Conference on Signal and Information Processing (GlobalSIP)*, IEEE, pp.584–588.

[10] **Zhang, J.**, **Wen, C.K.**, **Jin, S. and Li, G.Y.** (2019). Artificial Intelligence-Aided Receiver for a CP-Free OFDM System: Design, Simulation, and Experimental Test, *IEEE Access*, *7*, 58901–58914.

[11] **Balevi, E. and Andrews, J.G.** (2019). One-bit OFDM receivers via deep learning, *IEEE Transactions on Communications*.

[12] **Gao, X.**, **Jin, S.**, **Wen, C.K. and Li, G.Y.** (2018). ComNet: Combination of deep learning and expert knowledge in OFDM receivers, *IEEE Communications Letters*, *22*(12), 2627–2630.

[13] **Fang, L. and Wu, L.** (2017). Deep learning detection method for signal demodulation in short range multipath channel, *2017 IEEE 2nd International Conference on Opto-Electronic Information Processing (ICOIP)*, IEEE, pp.16–20.

[14] **Kim, M.**, **Kim, N.I.**, **Lee, W. and Cho, D.H.** (2018). Deep learning-aided SCMA, *IEEE Communications Letters*, *22*(4), 720–723.

[15] **O'Shea, T.J.**, **Erpek, T. and Clancy, T.C.** (2017). Deep learning based MIMO communications, *arXiv preprint arXiv:1707.07980*.

[16] **Xu, T. and Darwazeh, I.** (2019). Deep Learning for Over-the-Air Non-Orthogonal Signal Classification, *arXiv preprint arXiv:1911.06174*.

[17] **Zha, X.**, **Peng, H.**, **Qin, X.**, **Li, G. and Yang, S.** (2019). A Deep Learning Framework for Signal Detection and Modulation Classification, *Sensors*, *19*(18), 4042.

[18] **Farsad, N. and Goldsmith, A.** (2017). Detection algorithms for communication systems using deep learning, *arXiv preprint arXiv:1705.08044*.

[19] **Zhao, Z.**, **Vuran, M.C.**, **Guo, F. and Scott, S.** (2018). Deep-waveform: A learned OFDM receiver based on deep complex convolutional networks, *arXiv preprint arXiv:1810.07181*.

[20] **Turhan, M.**, **Ozturk, E. and Cirpan, H.** (2019). Deep learning aided generalized frequency division multiplexing, *Proc. 3rd Intl. Balkan Conf. Commun. Networking*.

[21] **Trubuil, J. and Chonavel, T.** (2012). Accurate Doppler estimation for underwater acoustic communications, *2012 Oceans-Yeosu*, IEEE, pp.1–5.

[22] **Hao, J.**, **Wang, J. and Song, J.** (2014). Joint channel and Doppler shift estimation in TDS-OFDM using frequency sensitive set, *2014 IEEE International Symposium on Broadband Multimedia Systems and Broadcasting*, IEEE, pp.1–4.

[23] **Yuan, G.**, **Wei, C.**, **Tao, X. and Biqi, L.** (2009). Doppler spread estimation for nonrayleigh fading channel, *2009 4th IEEE Conference on Industrial Electronics and Applications*, IEEE, pp.1106–1109.

[24] **Szegedy, C.**, **Liu, W.**, **Jia, Y.**, **Sermanet, P.**, **Reed, S.**, **Anguelov, D.**, **Erhan, D.**, **Vanhoucke, V. and Rabinovich, A.** (2015). Going deeper with convolutions, *Proceedings of the IEEE conference on computer vision and pattern recognition*, pp.1–9.

[25] **LeCun, Y.**, **Boser, B.**, **Denker, J.S.**, **Henderson, D.**, **Howard, R.E.**, **Hubbard, W. and Jackel, L.D.** (1989). Backpropagation applied to handwritten zip code recognition, *Neural computation*, *1*(4), 541–551.

[26] **Datta, R.**, **Michailow, N.**, **Lentmaier, M. and Fettweis, G.** (2012). GFDM interference cancellation for flexible cognitive radio PHY design, *2012 IEEE Vehicular Technology Conference (VTC Fall)*, IEEE, pp.1–5.

[27] **Arteaga, J.P.M.**, **David, R.P. and Neto, R.S.** (2017). Simultaneous detection and parallel interference cancellation in GFDM for 5G, *system*, *5*, 6.

[28] **Gaspar, I.**, **Matthé, M.**, **Michailow, N.**, **Mendes, L.L.**, **Zhang, D. and Fettweis, G.** (2015). Frequency-shift Offset-QAM for GFDM, *IEEE Communications letters*, *19*(8), 1454–1457.

[29] **Anwar, W.**, **Kumar, A.**, **Franchi, N. and Fettweis, G.** (2019). Performance Analysis using Physical Layer Abstraction Modeling for 5G and Beyond Waveforms, *IEEE Global Communications Conference (IEEE Globecom 2019)*.

CURRICULUM VITAE

Name Surname: Yasin YILDIRIM

Place and Date of Birth: Sivas , 12.11.1992

E-Mail: yildirimy17@itu.edu.tr

EDUCATION:

- **B.Sc.:** 2015, Istanbul University, Faculty of Engineering, Department of Electrical and Electronics Engineering

PROFESSIONAL EXPERIENCE AND REWARDS:

- **2018-... :** Research Assistant, *Department of Telecommunications Engineering, Yildiz Technical University*

- **2018-... :** Graduate Researcher, *Wireless Communication Research Laboratory, Istanbul Technical University*

PUBLICATIONS, PRESENTATIONS AND PATENTS ON THE THESIS:

- Deep Receiver Design for Multi-carrier Waveforms Using CNNs Y. Yildirim, S. Ozer, H.A. Cirpan 43rd IEEE International Conference on Telecommunications and Signal Processing (TSP), July 2020 (accepted).